Design Guidelines for RPC Prestressed Concrete Beams

Technical Report · May 2000

CITATIONS
47

READS
2,382

2 authors:

Nadarajah Gowripalan
University of Technology Sydney
70 PUBLICATIONS **1,283** CITATIONS

SEE PROFILE

R. I. Gilbert
UNSW Sydney
201 PUBLICATIONS **4,742** CITATIONS

SEE PROFILE

Design Guidelines for Ductal Prestressed Concrete Beams

N Gowripalan and R I Gilbert
School of Civil and Environmental Engineering
The University of New South Wales

May 2000

VSL

Ductal®

REFERENCE ARTICLE:

Design Guidelines for Ductal Prestressed Concrete Beams

Prof. Gowripalan N

Prof. Ian R Gilbert
Professor of Civil Engineering

School of Civil and Environmental Engineering, The University of NSW
May 2000: pp 53.

PREFACE:
This document was prepared for and on behalf of VSL (Aust) Pty Ltd. Its aim is to provide guidelines for the design of prestressed concrete beams using the Reactive Powder Concrete known as DUCTAL. Where possible, the design guidelines are consistent with the limit states design philosophy of AS3600-1994.

The authors have attempted to follow a first principles approach, based on well established principles of structural mechanics and the material properties and behaviour reported in the literature. In doing so, the authors have relied heavily on the results of research published overseas.

For comments please write to: ductal@vsl-australia.com.au

Alternatively please contact one of our Ductal experts for further information:

Brian Cavill FIEAust CPEng
Brian has been with VSL for more than 30 years, with responsibility for the manage-ment of their design activities and for the development of new technologies. He is a main driving force behind VSL's innovative concrete products, including Ductal.
bcavill@vsl-australia.com.au

Dr Mark Rebentrost
Mark joined VSL in 2004 after working for a major engineering consultant as a bridge designer. He has a PhD in non-linear structural engineering methods. His area of expertise at VSL includes the engineering of cost-effective and innovative Ductal solutions.
mrebentrost@vsl-australia.com.au

PREFACE

This document was prepared for and on behalf of VSL (Aust) Pty Ltd. Its aim is to provide guidelines for the design of prestressed concrete beams using the Reactive Powder Concrete known as DUCTAL. Where possible, the design guidelines are consistent with the limit states design philosophy of AS3600-1994. The authors have attempted to follow a first principles approach, based on well established principles of structural mechanics and the material properties and behaviour reported in the literature. In doing so, the authors have relied heavily on the results of research published overseas.

DISCLAIMER

TABLE OF CONTENTS

NOTATION

a a dimension of critical shear perimeter;
A area of cross-section;
A_m area enclosed by median lines of the walls of a hollow section;
A_p area of prestressing steel;
b width of section;
b_w width of web;
minimum wall thickness of a hollow section;
c cover;
C compressive force;
C_1, C_2 compressive force components in concrete;
d effective depth from the extreme compressive fibre to the resultant tensile force in the tensile zone at the ultimate limit state;
d_n depth to the neutral axis on the cracked section;
d_p depth to the prestressing steel;
D overall depth of the cross-section;
E_c elastic modulus of concrete at 28 days;
E_{cp} elastic modulus of concrete at transfer;
E_p elastic modulus of prestressing steel;
f_{cu} maximum compressive stress in concrete;
f'_c characteristic compressive strength at 28 days;
f'_{ct} characteristic flexural tensile stress at first cracking;
f'_{cp} characteristic compressive strength at transfer;
f_m mean compressive strength
f_{pu} ultimate tensile strength of prestressing steel;
HLP heavy load platform;
I second moment of area about centroidal axis;
I_g second moment of area of gross section;
J_t torsional constant;
k_u ratio of neutral axis depth to effective depth at the ultimate moment ($=d_n / d$);
L_{ef} effective span;
L_f length of fibre;
M moment;
M_i initial moment;
M_{max} maximum moment;
M_u ultimate moment;
M^* design moment for the ultimate limit state;
M_v^* moment transferred to a support;
P prestressing force;
P_e effective prestressing force after all losses;
P_i prestressing force immediately after transfer;
P_v vertical component of prestress;
Q first moment of area;
RPC reactive powder concrete;
R_u ultimate strength;
sd standard deviation;
SLS serviceability limit state;
S^* factored design action
T tensile force or torsion;
T_c tensile force in concrete;
T_p tensile force in prestressing steel;
T_u ultimate torsional strength;
T_{uc} torsional strength of concrete section;
T^* the design torsion (ULS)
T_1, T_2, T_3 tensile force components in concrete;
u perimeter length of critical section for punching shear;
ULS ultimate limit state;
V_t design shear force at the critical section;
V_u ultimate shear strength;
V_{uo} ultimate shear strength under a concentrated load;
V_{uc} shear strength contributed by concrete;
V_{us} shear strength contributed by stirrups;
V^* the design shear force (ULS);
w design crack width;
x shorter dimension of rectangular section;
X_1, X_2, X_3 distances;
y distance from centroidal axis;
longer dimension of rectangular section;
Z section modulus;
Z_b, Z_t section moduli with respect to bottom and top fibres, respectively;
χ aging coefficient;
ε strain;
ε_b strain in extreme tensile fibre;
$\varepsilon_{b,u}$ strain in bottom fibre at the ultimate limit state;
ε_{ce} concrete strain at steel level due to prestress;
ε_{cp} strain in the concrete at the tendon level;
ε_{pt} strain component in prestressing steel;
ε_o top fibre strain;
$\varepsilon_{o,u}$ top fibre strain at ultimate limit state;
$\varepsilon_{t,p}$ limiting tensile strain in concrete (Fig 5);
$\varepsilon_{t,u}$ limiting tensile strain in concrete (Fig 5);
ε_{sh}^* final shrinkage strain;
ϕ strength (or capacity) reduction factor;
ϕ^* final creep coefficient;
κ curvature;
κ_i instantaneous curvature;
κ_m curvature at midspan;
κ_s curvature at support;
σ stress;
σ_{cp} average prestress after all losses, P_e/A;
σ_o top fibre concrete stress after cracking;
σ_{bot} stress in concrete in bottom fibre;
σ_{top} stress in concrete in top fibre;
σ_1 principal tensile stress;
τ shear stress;
Δ deflection;
$\Delta\sigma_p$ loss of prestress;

1. INTRODUCTION

This document provides guidelines for the design of prestressed concrete beams manufactured using the Reactive Powder Concrete (RPC) known as *Ductal*. Where possible, a limit states approach consistent with the design requirements of the Australian Standard for Concrete Structures AS3600 – 1994 has been adopted.

Reactive Powder Concrete is a relatively new material and research into the properties and behaviour of RPC is still in its infancy. Most existing literature on RPC, and it structural applications, is written in French and efforts have been made to study these documents, together with the relevant French design codes and specifications. Currently available literature indicates that RPC can readily be used in a wide variety of structural applications, including bridges, highway structures, pipes, culverts and precast members. For prestressed concrete applications, RPC appears to be an ideal construction material.

The design guidelines presented here are based on a study of the existing literature, research undertaken at UNSW and elsewhere and information gained from the performance of existing RPC structures constructed overseas. The guidelines are necessarily based on the current state of knowledge and, where possible, a *first principles* approach has been adopted. The design procedures have been developed based on the principles of structural mechanics and the material properties and behaviour reported in the literature. Research is continuing in many areas and, as more information becomes available, sections of the document will be improved and re-calibrated and, no doubt, the document will be expanded. However, in order to facilitate design of prestressed girders manufactured from *Ductal*, detailed design rules and recommendations have been made. In some areas, design guidance is provided, but it is based on the authors' experience rather than on well-documented and independently verified research. Numerical examples illustrating the behaviour of pretensioned concrete beams and unreinforced elements are included in the Appendices, together with detailed design calculations for pretensioned bridge girders.

2. SCOPE AND APPLICATION

This document sets out guidelines for the design of prestressed concrete beams manufactured from the Reactive Powder Concrete (RPC) known as *Ductal*. The beams are prestressed longitudinally with steel tendons. The guidelines include the design of the non-prestressed elements of the beam transverse to the direction of the prestress (including overhanging flanges and transverse ribs, if any).

Ductal is a material developed by Bouygues, S.A., Paris and made from particles smaller than 800μm (hence the name *powder concrete*). By replacing coarse aggregate with fine sand,

the size of the microfissures linked to intrusions in traditional concrete is greatly reduced. *Ductal* contains large quantities of a particular steel fibre. The presence of the steel fibres is essential to enhance the post-cracking tensile strength and to improve the ductility of the material. A typical mix for *Ductal* resulting in a mean cylinder compressive strength of 228 MPa and a characteristic compressive strength of 197 MPa is given in Table 1. Additional information on *Ductal* is provided in Appendix A.

Table 1 Typical composition of *Ductal* (Dallaire et al., 1998).

Component Material	Quantity (kg/m^3)
Cement	705
Silica fume	230
Crushed quartz	210
Sand	1010
Superplasticizer	17
Steel fibres	190
Water	195

The guidelines are intended to apply to prestressed structural members made of DUCTAL with

(a) a characteristic compressive strength at 28 days, f_c', in the range 150 to 220 MPa;

(b) a minimum fibre content of 2.0% by volume (the fibre length is 13mm and diameter is 0.2mm) with a minimum fibre tensile strength of 1800 MPa;

(c) a saturated, surface-dry density in the range 2400 kg/m^3 to 2650 kg/m^3; and

(d) sufficient curing to develop a minimum characteristic strength at transfer of 100 MPa and a minimum elastic modulus at transfer of 40000 MPa.

An initial heat treatment, consisting of curing in hot water or steam at a temperature of 90°C for a period not less than 48 hours, substantially reduces the creep of *Ductal* and causes almost all the shrinkage to occur during the period of heat treatment.

It is intended that these design guidelines are to be used by a competent, experienced and suitably qualified engineer (a person qualified for Corporate Membership of the Institution of Engineers, Australia, or with equivalent qualifications, and competent to practise in the design and construction of concrete structures).

3. DESIGN REQUIREMENTS AND PROCEDURES

3.1 Requirements:

In the design of a prestressed concrete beam, the aim is to provide an element that is durable, serviceable and has adequate strength to fulfil its intended function. It must also be robust, have adequate fatigue resistance and satisfy other relevant requirements, such as ease of construction and economy.

A beam is durable if it withstands expected wear and deterioration throughout its intended life without the need for undue maintenance. It is serviceable and has adequate strength if the probability of loss of serviceability and the probability of collapse are both acceptably low throughout its intended life.

These guidelines, as far as possible, provide design requirements that are consistent with those in AS3600 – 1994.

3.2 Design for Strength:

Beams should be designed for strength as follows:

(a) The loads, other actions and the 'design load for strength' are determined in accordance with Section 3 of AS3600.

(b) The design action effect, S^*, due to the design load for strength is determined by an appropriate analysis.

(c) The design strength, ϕR_u, is determined as outlined in Section 5.1 of this document, where ϕ is a strength reduction factor and R_u is the ultimate strength. For elements where flexural strength is provided by bonded reinforcement or tendons, and the ductility requirements of Section 5.3 are satisfied, ϕ should not exceed 0.8 for bending and 0.7 for shear and torsion. For elements where flexural strength is not provided by bonded reinforcement or tendons, ϕ should not exceed 0.7.

(d) The beam is proportioned so that its design strength is greater than or equal to the design action effect, ie. $\phi R_u \geq S^*$.

3.3 Design for Serviceability:

Beams should be designed for serviceability by controlling or limiting deflection, cracking and vibration, as appropriate, in accordance with the requirements of Section 2.4 in AS3600.

The deflection of a beam under service conditions should be controlled as follows:

(a) a limit for the calculated deflection is chosen appropriate to the support conditions and the intended use. AS3600 provides the following deflection limits.

Type of member	Deflection to be considered	Deflection limitation (Δ/L_{ef}) for spans	Deflection limitation (Δ/L_{ef}) for cantilevers
All members	The total deflection	1/250	1/125
Members supporting masonry partitions or other brittle finishes	The deflection which occurs after the addition or attachment of the partitions or finishes	1/500 where provision is made to minimize the effect of movement, otherwise 1/1000	1/250 where provision is made to minimize the effect of movement, otherwise 1/500
Bridge members	The live load (and impact) deflection	1/800	1/400

(b) the member should be designed so that, under the 'design load for serviceability' (determined in accordance with Section 3 of AS3600), the calculated deflection does not exceed the limit selected in (a) above.

The cracking of a beam under service conditions should be controlled, with limits on crack width being selected to ensure acceptable appearance and durability.

The vibration of a beam under service conditions should be such that it does not adversely affect the serviceability of the structure. Vibrations due to machinery, or vehicular or pedestrian traffic, should be considered where applicable. To minimise vibration of beams, the additional deflection due to live loads alone may be limited to Span/800.

3.4 Design for Durability:

Beams should be designed for durability in accordance with the general requirements of Section 4 of AS3600. However, the durability of *Ductal* is superior to high performance (conventional) concrete. The porosity of *Ductal* is about 5% and, hence, its permeability is very low. Steel fibre reinforced concrete with a dense cementitious matrix has outperformed other types of concrete, even in a marine environment.

For exposure classifications A1, A2, B1, B2 and C, the minimum required cover of well compacted *Ductal* to the tendons is 20 mm and the minimum clear spacing between adjacent tendons is 1.5 times the tendon diameter or 20 mm, whichever is the larger.

4. DESIGN PROPERTIES OF DUCTAL

4.1 Behaviour in Compression

A typical stress-strain curve for Ductal is shown in Figure 1. The curve was obtained from measurements taken in a standard compression test on a 70 mm diameter cylinder (Behloul, 1999). The ascending part of the stress-strain curve OA is essentially linear up to the peak stress, f_{cu}. On reaching the peak stress, the steel fibres provide considerable ductility, as is evidenced by the plateau AB in Figure 1. The extent of the plateau depends on the type and quantity of steel fibres. The shape of the post-peak, descending part of the stress-strain curve also depends on the type and quantity of steel fibres.

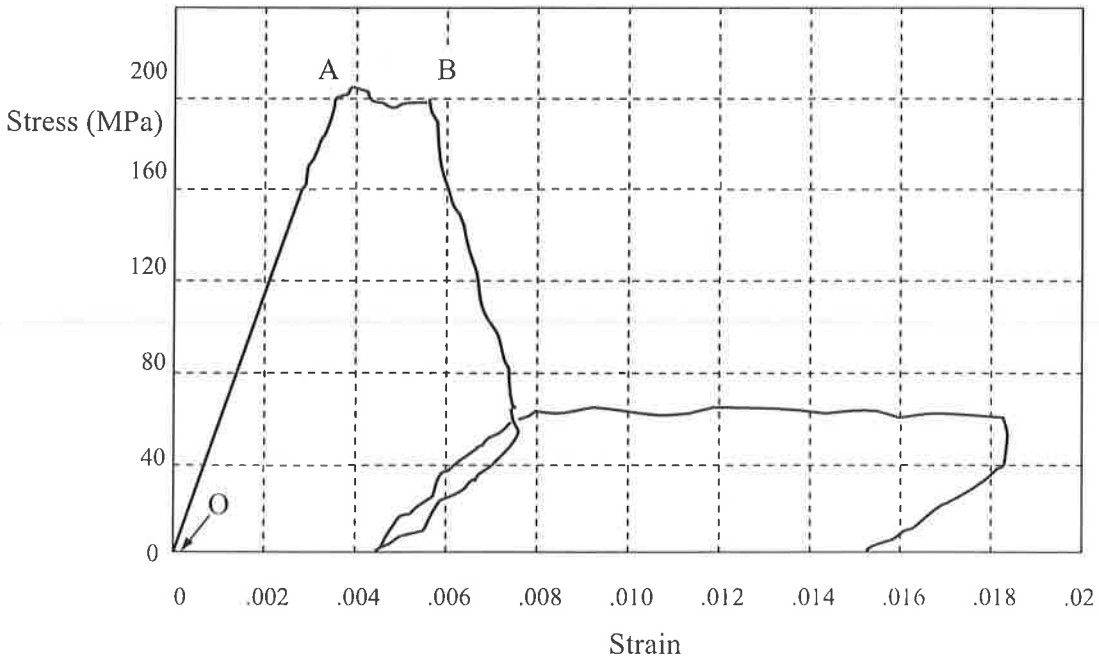

Figure 1 Typical stress-strain relationship in compression (Behloul, 1999).

4.2 Characteristic Compressive Strength

The characteristic compressive strength of RPC, f_c', should be determined statistically from compressive strength tests in accordance with AS1012.9.

In order to obtain the specified characteristic strength f_c', the following equation can be used:

$$f_c' = f_m - 2.33\, sd \qquad (4.1)$$

where f_m is the mean compressive strength and sd is the standard deviation.

The characteristic compressive strength, f_c', is obtained from standard 28 day compressive tests on carefully prepared cylinders with the ends cut or ground square. The diameter of the cylinders may vary between 70 and 100 mm and the length of the cylinders is twice the diameter.

4.3 Idealised Stress-Strain Relationship in Compression

For design purposes, the idealised stress-strain relationship shown in Figure 2 may be used.

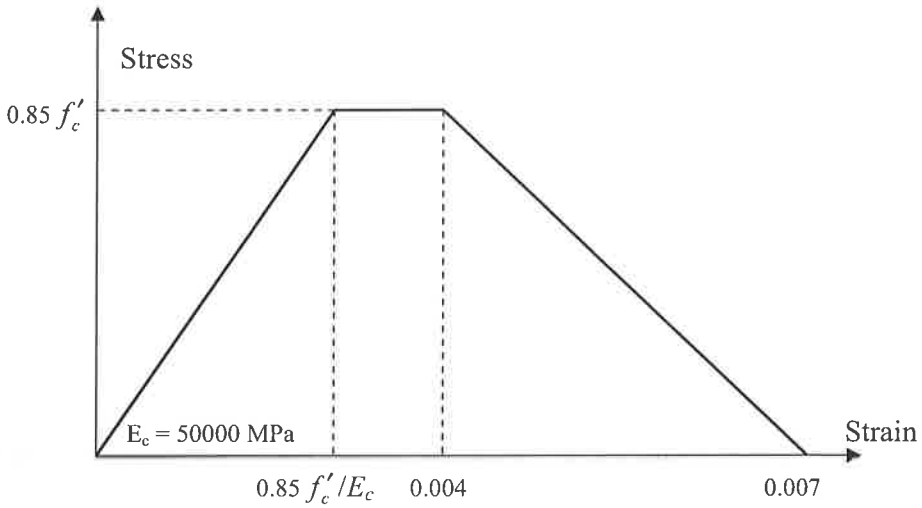

Figure 2 Design stress-strain relationship in compression

4.4 Behaviour in Tension

The tensile strength of *Ductal* is variable and the behaviour after cracking is highly dependent on the type, quantity and orientation of steel fibres crossing the crack. Typical results of a direct tensile tests conducted on a 70 mm diameter notched *Ductal* cylinder are shown in Figure 3, together with the range of variability to be expected. A significant observation to be made from Figure 3 is that the average tensile stress on the cracked surface actually increases after first cracking, before beginning to decrease at a crack width of about 0.2mm. As the crack width increases some of the fibres crossing the crack pull-out of the crack surface and the average tensile stress decreases.

The flexural tensile strength of *Ductal* is higher than the direct tensile strength with values in excess of 40 MPa (M_{max}/Z) having been recorded. After cracking, the tension carried across the crack depends on the crack width, the quantity and type of fibres crossing the crack and the depth of the beam, D. Since the quantity of fibres crossing the crack will inevitably vary from one crack

to another, a high factor of safety is recommended in design when estimating the tension carried across a crack.

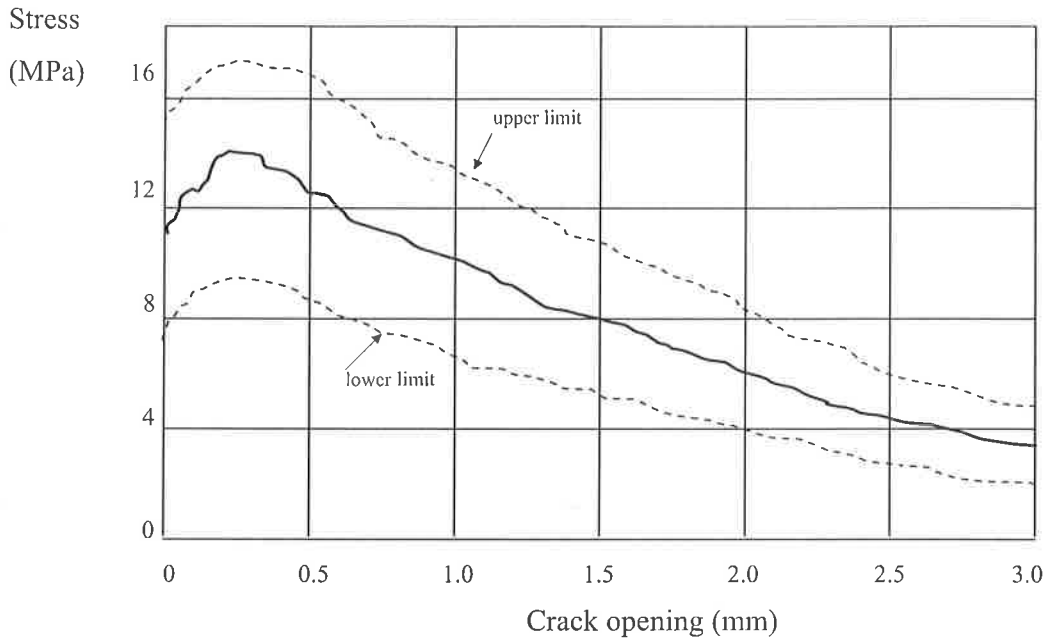

Figure 3 Behaviour in direct tension (Behloul,1999)

The characteristic flexural tensile strength, f'_{cf}, may be determined statistically from standard three point or four point modulus of rupture tests on prisms of square section using a formula similar to Eqn 4.1. Unlike conventional concretes, the maximum moment (M_u) carried by a prism of *Ductal* in a standard modulus of rupture test is considerably higher than the moment required to cause first cracking (M_{cr}). The flexural tensile strength ($f_{cf} = M_u/Z$) is therefore higher than the tensile stress at the onset of cracking ($f_{ct} = M_{cr}/Z$). Since M_u is generally greater than $1.2M_{cr}$ for an unreinforced *Ductal* flexural member, the minimum flexural reinforcement requirements for conventional concrete flexural members are not required for *Ductal* elements.

Overseas practice (Behloul, 1999) is to reduce the measured modulus of rupture by a factor of safety of about 4 when determining the design tensile stress at which cracking first occurs. For the range of *Ductal* strengths considered in this document ($150 \le f'_c \le 220$ MPa), the characteristic flexural tensile stress at which cracking is initiated may be taken as

$$f'_{ct} = 8.0 \text{ MPa} \qquad (4.2)$$

After cracking, the stress-strain curve for concrete in tension depends on the fibre length, L_f, the fibre content and the depth of the beam, D. For a fibre length of $L_f = 13$ mm and a fibre content of 2% by volume, the stress-strain curves for concrete in tension for various beam depths are shown in Figure 4 (Behloul, 1999). The ascending part of these curves is linear with a slope corresponding to an elastic modulus of 50 GPa. The descending curve may be approximated by a

third order polynomial (Behloul, 1999) with the stress equal to zero when the strain reaches $\varepsilon_{t,u}$. According to Behloul (1999), $\varepsilon_{t,u} = L_f / 1.2D$.

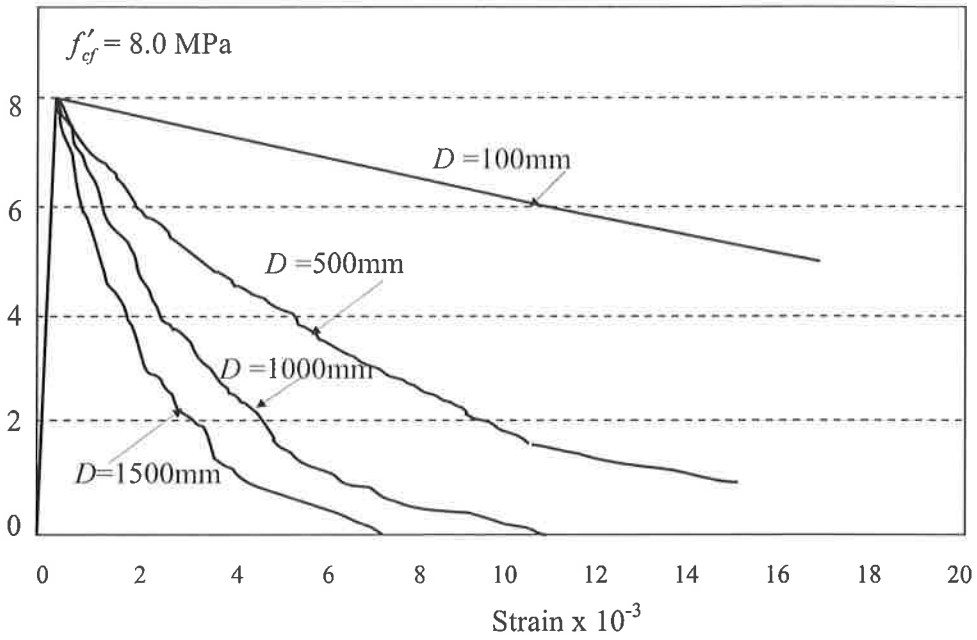

Figure 4 Stress-strain relationships for Ductal in tension (Behloul, 1999).

4.5 Idealised stress-strain relationship in tension

For design purposes, the idealised stress strain relationship shown in Figure 5 may be used to determine behaviour in the post cracking range. D is the overall depth of the beam and L_f is the length of the fibres.

4.6 Modulus of Elasticity

For design calculations, a modulus of elasticity of 50GPa (after 28 days) and 40 GPa at transfer may be used.

4.7 Density

The density of RPC varies between 2400 kg/m^3 and 2650 kg/m^3. It should be determined based on mix composition or by testing.

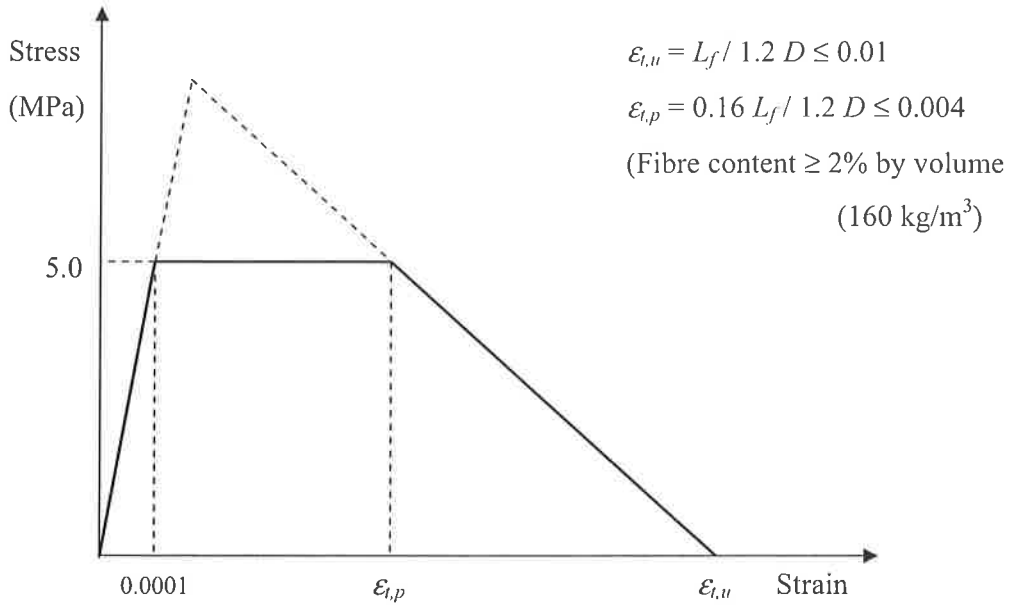

Figure 5 Design stress-strain relationship in tension.

4.8 Poisson's Ratio

Poisson's Ratio of RPC varies between 0.16 and 0.24 (Behloul, 1996). This is similar to the typical values obtained for conventional concretes. In the absence of any test results, a value of 0.2 may be used for calculations.

4.9 Creep

As for conventional concretes, the creep of *Ductal* depends on the age at first loading and the duration of the applied stress. It also depends on the period of curing and the temperature during curing. Reactive powder concrete initially cured at 90°C for 48 hours exhibits very little creep, with a final creep coefficient ϕ^* of about 0.3 (when first loaded at 28 days). The final creep coefficient is the ratio of creep strain to initial elastic strain. If the RPC is not steam cured then ϕ^* can be as high as 1.2 for specimens loaded at 28 days and 1.80 for specimens loaded at 4 days. Figure 6 shows a typical set of elastic plus creep strain (per unit of stress) versus time curves for *Ductal* loaded at different ages. Recommended values of ϕ^* for use in design are as follows:

Time of first loading	Final creep coefficient, ϕ^*	
	Without steam curing	With steam curing for 48hrs
4 days	1.8	0.5
28 days	1.2	0.3

4.10 Shrinkage

Reactive powder concrete suffers an endogenous shrinkage strain of about 500 x 10^{-6}. If initially subjected to steam curing at 90°C for at least 48 hours, almost all the shrinkage occurs during the period of steam curing, with no shrinkage taking place subsequently. If cured at room temperatures, the shrinkage takes place over a considerably longer period increasing at a decreasing rate, as shown in Figure 7. The shrinkage is essentially the result of chemical reactions within the RPC and is not the same as drying shrinkage in conventional concretes. As a result, even for RPC cured at room temperatures, the great majority of shrinkage occurs in the first 28 days after casting.

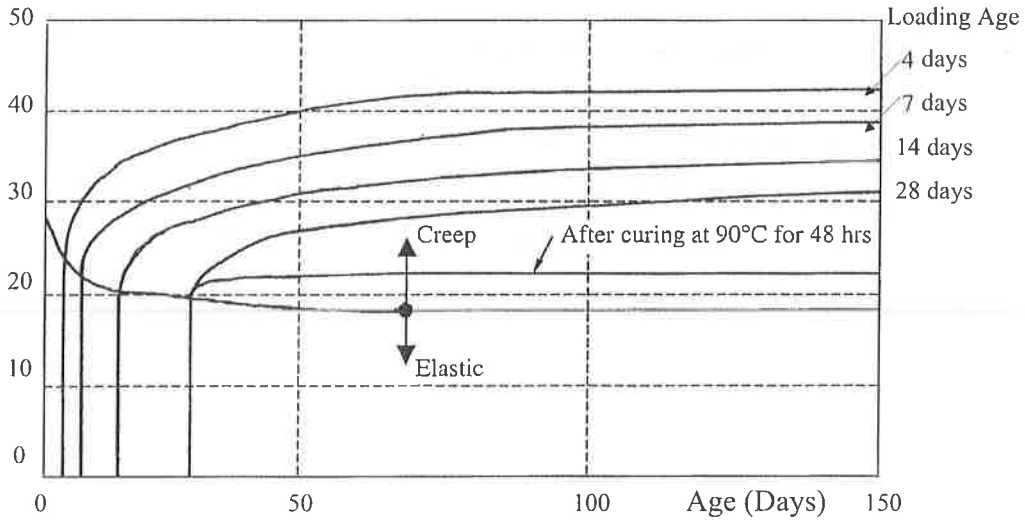

Figure 6 Creep plus elastic strain versus time (Behloul, 1999)

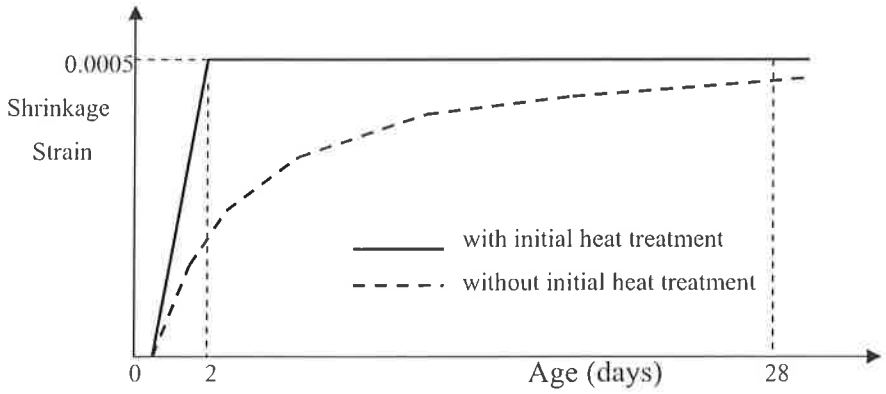

Figure 7 Shrinkage versus time for specimens with and without initial heat treatment.

5. STRENGTH IN FLEXURE

5.1 Theoretical Moment Capacity

Calculations for strength of a section in bending should incorporate equilibrium and strain compatibility considerations and be consistent with the following assumptions:

(a) plane sections normal to the beam axis remain plane after bending; and

(b) the distribution of concrete compressive and tensile stresses are as outlined in Figures 2 and 5, respectively.

Typical stress and strain distributions at the ultimate limit state for a singly reinforced cross-section (ie. a cross-section containing a single layer of bonded tendons) and for a cross-section containing no bonded reinforcement are shown in Figures 8 and 9, respectively.

For a prestressed section containing bonded tendons in the tensile zone (such as that shown in Figure 8) at the ultimate limit state in bending, the extreme fibre compressive strain may be taken as $\varepsilon_{o,u} = 0.0035$.

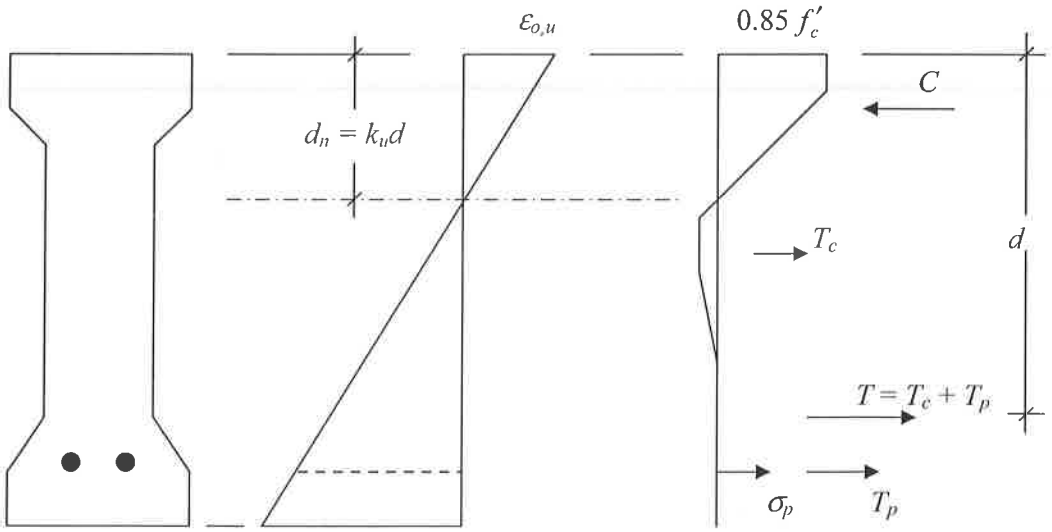

Figure 8 Stress and strain distributions at the ultimate bending limit state for a cross-section containing bonded tendons

For a section containing no bonded reinforcement or tendons (such as that shown in Figure 9), the ultimate strength in bending may be assumed to occur when the extreme fibre tensile strain ($\varepsilon_{b,u}$ in Figure 9) equals $\varepsilon_{t,p}$ (as defined in Figure 5).

The design strength in bending is obtained by multiplying the calculated ultimate strength M_u by the strength reduction factor, ϕ. For a cross-section containing bonded reinforcement or

tendons (as in Figure 6), when $k_u \leq 0.4$, $\phi = 0.8$. For a cross-section containing no bonded reinforcement or tendons in the tensile zone (as in Figure 9), where flexural strength after cracking is provided by the steel fibres, $\phi = 0.7$.

Sections containing bonded reinforcement or tendons in which $k_u > 0.4$ are likely to fail in a brittle manner and should not be used.

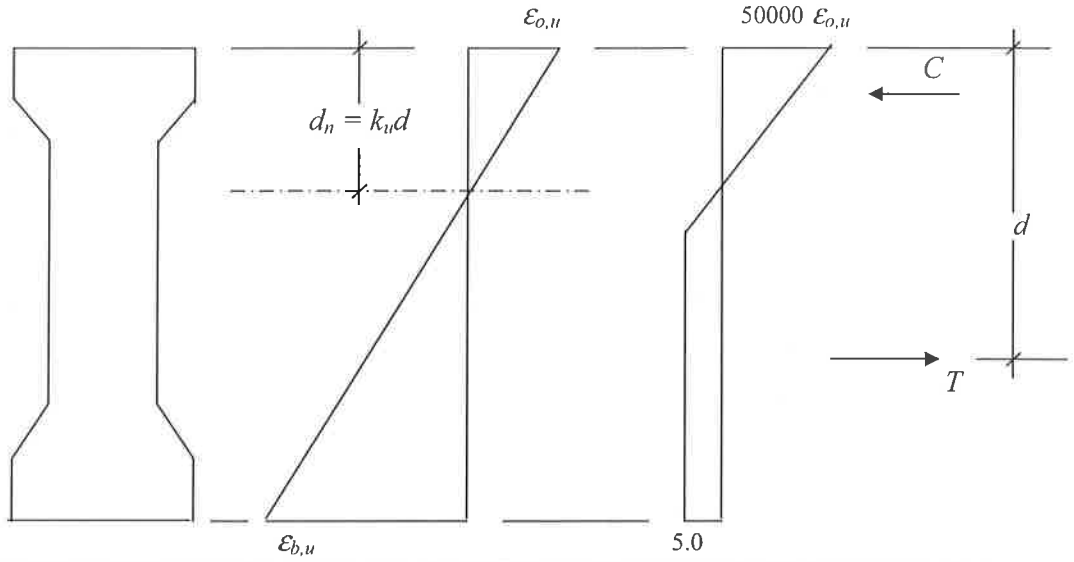

Figure 9 Stress and strain distributions at the ultimate bending limit state for a cross-section containing no bonded tendons

5.2 Minimum Strength and Other Requirements:

The ultimate strength in bending should be greater than 1.2 times the cracking moment. The cracking moment is the moment that produces a tensile stress equal to f'_{cf} in the extreme concrete tensile fibre of the uncracked section. This requirement may be waived if the design ultimate bending moment M* is less than 0.5 times the cracking moment.

To avoid premature local buckling of slender elements in a cross-section, the ratio of effective length to thickness of flanges or webs should be less than 25 when the flange or web is supported at both ends or 10 when the flange or web outstand is supported at one end only.

5.3 Ductility Requirements

The ductility of a cross-section in bending depends on the deformation (or curvature) at failure and hence the ratio of the neutral axis depth to the effective depth of the cross-section, k_u. The effective depth d is the distance from the extreme compression fibre of the concrete to the resultant tensile force in the tendons, reinforcing steel (if any) and steel fibres in that zone which will be tensile at the ultimate strength condition in pure bending (as shown in Figures 8 and 9).

Hence, k_u is affected by the quantity of reinforcement in the tensile zone (which includes tendons, conventional reinforcement and fibres).

To ensure adequate ductility, k_u should not exceed 0.4.

6. STRENGTH IN SHEAR

6.1 Discussion

The existing French literature suggests that the design for shear requires checks at both the serviceability and ultimate limit states. For serviceability, shear can only be a problem if it causes cracks under service loads with widths exceeding acceptable crack limits. The approach taken here when checking the shear strength of sections not containing transverse shear reinforcement will ensure that shear cracking under service conditions does not occur. Hence, the design for shear need only consider the strength limit states.

6.2 Design Shear Strength

The design shear force V^* (caused by the factored design loads for the strength limit states) should not exceed the design strength, ϕV_u (where $\phi = 0.7$ in accordance with AS3600 – 1994).

The shear strength of a prestressed concrete section, V_u, is given by

$$V_u = V_{uc} + V_{us} + P_v \tag{6.1}$$

where V_{uc} is the contribution of the concrete to the shear strength, V_{us} is the contribution of the transverse shear reinforcement (if any) and P_v is the transverse component of the prestressing force which will exist if the prestressing tendon is inclined at an angle to the member axis.

In the absence of shear reinforcement and inclined tendons, for pretensioned beams, the shear strength becomes

$$V_u = V_{uc} \tag{6.2}$$

Much more research is required to calibrate the post-cracking contribution of RPC to the shear strength of beams. At present, it is suggested that, for a cross-section that is uncracked in flexure, the shear strength V_{uc} is limited to the shear force V_t required to produce a principal tensile stress of $(5.0 + 0.13\sqrt{f_c'})$ (in MPa) at either the centroidal axis or at the junction of the web and the flange of the cross-section, whichever is the smaller.

The stresses at a point in the web of a cross-section are shown in Figure 10.

Figure 10

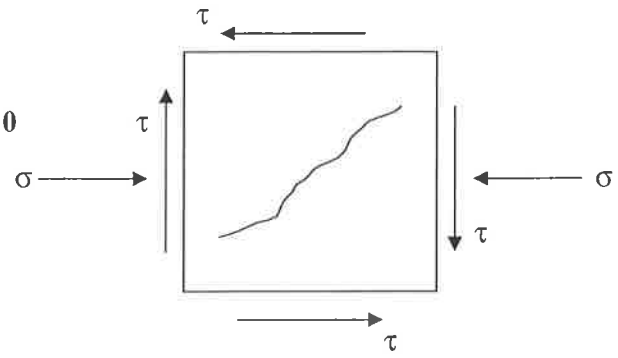

The principal tensile stress σ_1 is given by

$$\sigma_1 = \frac{\sigma}{2} + \sqrt{\left(\frac{\sigma}{2}\right)^2 + \tau^2} \qquad (\leq (5.0 + 0.13\sqrt{f_c'})\ \text{MPa}) \qquad (6.3)$$

where $$\sigma = -\frac{P}{A} - \frac{Pe\,y}{I} + \frac{My}{I} \qquad \text{and} \qquad \tau = \frac{V_t Q}{Ib} \qquad (6.4)$$

P is the effective prestress after all losses; e is the eccentricity of the prestressing tendon; y is the distance from the centroidal axis to the point under consideration; A and I are respectively the area of the cross-section and the second moment of area of the cross-section about the centroidal axis; Q is the first moment of area about the centroidal axis of that part of the cross-section between the level under consideration and the extreme fibre; b is the width of the web at the point under consideration; and M is the moment at the section when the shear force is V_t. With V_t calculated from Eqn 6.3, the shear strength of a section not containing stirrups may be taken as

$$V_{uc} = V_t + P_v \qquad (6.5)$$

6.3 Critical Section for Shear in Beams

When a beam is supported on its soffit and diagonal cracking cannot take place at the support or extend into the support, the critical section for shear is at a distance equal to d from the face of the support. Where diagonal cracking can take place at the support or extend into the support, the critical section is at the face of the support. The maximum transverse shear to be considered in design is the factored design ultimate shear force at the critical section.

6.4 Strength of Slabs in Shear

The strength of a slab in shear shall be determined in accordance with the following:

(a) Where shear failure can occur across the width of the slab, the design shear strength of the slab shall be calculated in accordance with Section 6.2.

(b) Where shear failure can occur locally around a support or concentrated load, the design shear strength of the slab shall be taken as ϕV_u, where V_u is calculated from

$$V_u = \frac{V_{uo}}{[1+\frac{uM_v^*}{8V^*ad}]} \tag{6.6}$$

where

$$V_{uo} = ud(5+0.3\sigma_{cp}) \tag{6.7}$$

and u is the effective length of the critical shear perimeter; M_v^* is the bending moment transferred from the slab to the support in the direction being considered; d is the effective depth of the slab averaged around the critical shear perimeter; a is the dimension of the critical shear perimeter measured parallel to the direction of the span producing M_v^*; and σ_{cp} is the average effective prestress around the critical shear perimeter (+ve if compressive and -ve if tensile).

The critical shear perimeter, mentioned in (b) above, is defined by a line geometrically similar to the boundary of the effective area of a support or concentrated load and located at a distance of $d/2$ therefrom.

In the case of a concentrated wheel load acting on a slab, M_v^* is zero and Eqns 6.6 and 6.7 reduce to

$$V_u = V_{uo} = ud(5+0.3\sigma_{cp}) \tag{6.8}$$

7. STRENGTH IN TORSION

7.1 Design Torsional Strength

For a member or element subjected to pure torsion, the design torsion T^* (caused by the factored design loads for the strength limit states) should not exceed the design strength, ϕT_u, where $\phi = 0.7$ in accordance with AS3600 – 1994.

For a member **not** containing torsional reinforcement (in the form of closed ties and longitudinal reinforcement), the torsional strength T_u may be taken as the torsional strength of the concrete section, T_{uc}, which is conventionally taken as the pure torsion required to cause first cracking and may be estimated from Eqn 7.1.

$$T_{uc} = J_t \ (5.0 + 0.13\sqrt{f_c'}) \ \sqrt{1 + 10\sigma_{cp} / f_c'} \qquad (7.1)$$

where J_t is the torsional constant for the cross-section given by

$J_t = 0.4x^2 y$ for solid sections

$= 0.4\Sigma x^2 y$ for solid flanged sections

$= 2A_m b_w$ for thin-walled hollow sections

x and y are the shorter and longer overall dimensions of the rectangular part(s) of the solid section, respectively; A_m is the area enclosed by the median lines of the walls of a hollow section; bw is the minimum thickness of the walls of the hollow section; the term $(5.0 + 0.13\sqrt{f_c'})$ represents the tensile strength of the concrete in MPa; the term $\sqrt{1 + 10\sigma_{cp} / f_c'}$ is the beneficial effect of the prestress; and σ_{cp} is the average effective prestress, P_e/A.

7.2 Strength in combined Shear and Torsion

For a cross-section subjected to combined shear and torsion and not containing shear or torsional reinforcement, the requirements for adequate strength are satisfied if the following inequality is satisfied:

$$\frac{T^*}{\phi T_{uc}} + \frac{V^*}{\phi V_{uc}} \le 0.75 \qquad (7.2)$$

where T^* and V^* are the factored design torsion and shear, respectively; T_{uc} is determined from Eqn 7.1; and V_{uc} is obtained from Eqn 6.5. Much more research is required to calibrate the strength of RPC beams in combined shear and torsion. The procedure adopted here is consistent with the procedure taken in AS3600 and is considered to be adequate.

8. CRACK CONTROL IN FLEXURE AT SERVICE LOADS

8.1 Non-Prestressed Elements

Flexural cracking may be deemed to be controlled, if under the short-term service loads the resulting maximum tensile stress in *Ductal* does not exceed 6.0 MPa.

If flexural cracking does occur under short-term service loads, the cracks may be deemed to be controlled if the design crack width at the extreme tensile fibre is less than 0.3mm. In the case of a cross-section not containing any bonded tendons in the tensile zone, the design crack width, w, at the extreme tensile fibre of the section may be taken as

$$w = 1.5D(\varepsilon_b - 0.00016) \qquad (8.1)$$

where ε_b is the concrete strain at the extreme tensile fibre calculated from a cracked section analysis.

8.2 Prestressed Elements

For sections containing bonded tendons in the tensile zone, flexural cracking may be deemed to be controlled if, under short-term service loads, the resulting maximum tensile stress in the concrete does not exceed 8.0 MPa, or if this stress is exceeded, by

(a) providing bonded reinforcement or tendons near the tensile face; and

(b) the increment in steel stress near the tension face is less than 200 MPa, as the load is increased from its value when the extreme concrete tensile fibre is at zero stress to the short-term service load value.

9. DEFLECTION AT SERVICE LOADS

9.1 Short-term deflection

Most RPC prestressed beams will be uncracked under service loads. The short-term deflection of uncracked beams may be calculated assuming an elastic modulus of 50000 MPa and the second moment of area of the gross section about the centroidal axis.

If cracking occurs under service loads, the instantaneous curvature, κ_i, at a cracked cross-section may be calculated assuming the stress distribution shown in Figure 11.

The short-term deflection may then be obtained by integrating the curvature at selected cross-sections along the beam.

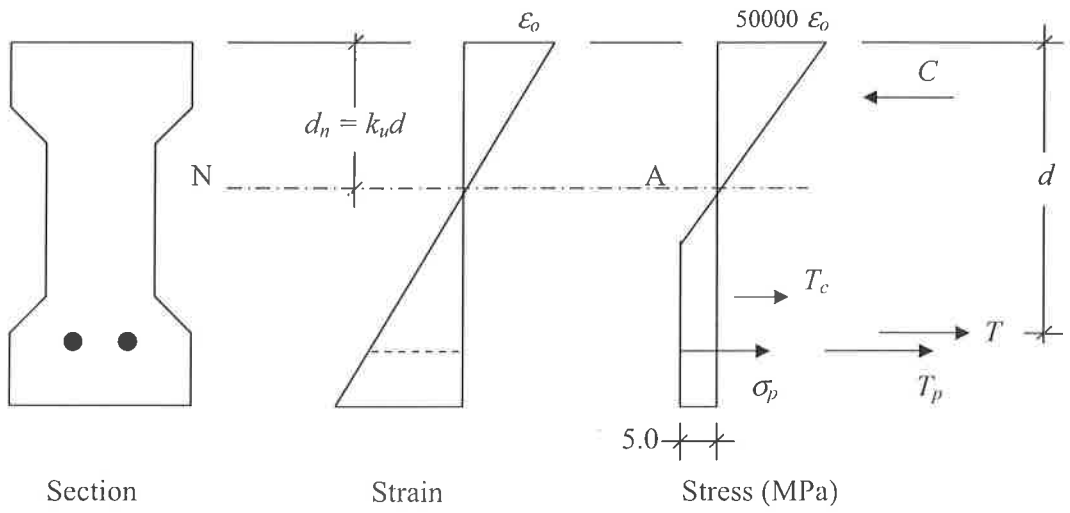

Figure 11 Stress and strain on a cracked section

9.2 Long-term deflection:

A reliable estimate of long-term deflection may be obtained by integrating the final curvatures obtained from time analyses of the critical cross-sections, using the well established age-adjusted effective modulus method (see Section 3.6 in Gilbert and Mickleborough, 1990).

For elements not subjected to initial heat treatment, it is suggested that a final creep coefficient in the range 1.2 – 1.8, an aging coefficient of 0.8 and a final shrinkage strain of -0.0005 be used in the analyses. For members subjected to initial heat treatment, a final creep coefficient in the range 0.3 - 0.5, an aging coefficient of 0.8 and a final shrinkage strain of -0.0001

should be used in the analyses. It should be remembered that an endogenous shrinkage strain of about -0.0005 occurs during the heat treatment process (in the first 48 hours).

10. RESISTANCE TO FIRE

The fire resistance of *Ductal* is currently the subject of research and no conclusive recommendations can be made. Some RPC mixes with 200MPa compressive strength, showed spalling at 500°C. Mix design is critical in achieving enhanced performance under fire conditions. A mix of steel and synthetic fibres has been shown to alleviate some of the problems by providing voids in the RPC which reduce the build up of internal pressure during exposure to fire.

However, in applications such as bridge beams and sound barriers this is not considered to be a problem. For building structures, the resistance to fire is more important and consideration should be given to the inclusion of synthetic fibres in the mix.

11. FATIGUE

Fatigue tests carried out on DUCTAL specimens indicate that RPC has a superior fatigue performance than normal strength concrete, high performance concrete and conventional reinforced concrete, as shown in Figure 12.

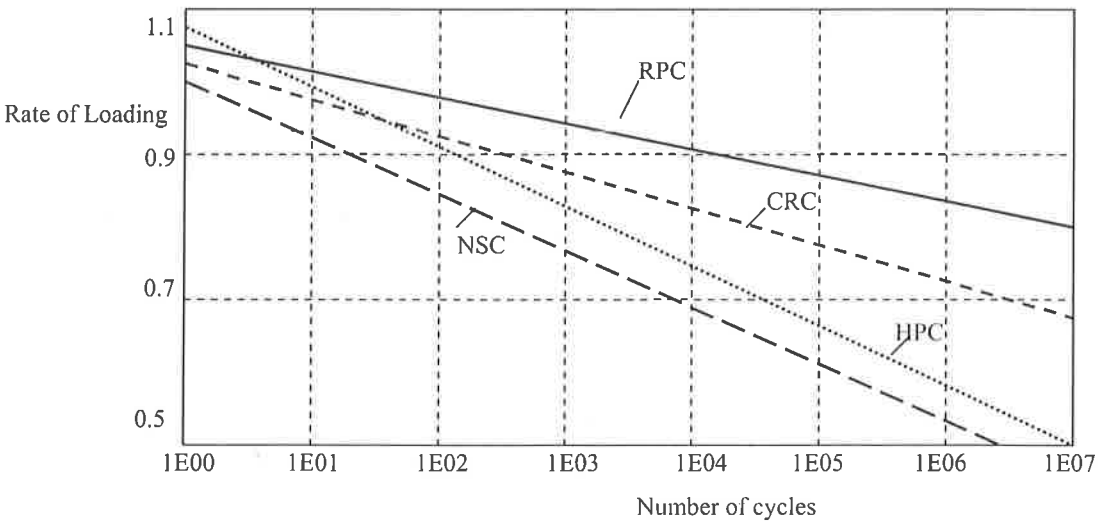

Figure 12 S-N curves (Behloul, 1999).

12. LOSSES OF PRESTRESS

12.1 Instantaneous losses:

When the prestress is transferred to the concrete in a pretensioned beam, instantaneous losses of prestress occur due to elastic shortening. The change in strain in the prestressing steel $\Delta\varepsilon_p$ caused by elastic shortening of the RPC is equal to the strain in the concrete at the steel level, ε_{cp}, and hence

$$\varepsilon_{cp} = \frac{\sigma_{cp}}{E_c} = \Delta\varepsilon_p = \frac{\Delta\sigma_p}{E_p} \tag{12.1}$$

The loss of stress in the steel is therefore

$$\Delta\sigma_p = \frac{E_p}{E_c}\sigma_{cp} \tag{12.2}$$

where σ_{cp} is the concrete stress at the steel level immediately after transfer.

If endogenous shrinkage (ε_{sh}) takes place between pouring the RPC and transfer, an additional loss of prestress will occur before transfer and may be taken as $\Delta\sigma_p = \varepsilon_{sh}E_p$.

12.2 Time-dependent losses:

Time-dependent losses of prestress will occur due to creep, shrinkage and relaxation of the steel tendons. A reliable estimate of these losses can be obtained from a time analysis of the cross-sections under consideration using the well established age-adjusted effective modulus method (see Section 3.6 in reference 6 (Gilbert and Mickleborough, 1990)).

The procedures specified in AS3600 for calculating the loss of prestress due to creep and shrinkage of the concrete overestimate losses, as they do not account for the reduction in compressive strains induced in the concrete at the steel level as the time-dependent losses take place. At best they provide an upper estimate of losses (and for this reason only they are outlined below), but generally they are misleading and should not be used.

AS3600 suggests that for a section containing no non-prestressed reinforcement the loss of prestress due to shrinkage may be taken as $\Delta\sigma_p = \varepsilon_{sh}E_p$ and the loss of prestress due to creep may be taken as $\Delta\sigma_p = (\sigma_c / E_c)\ \phi\ E_p$, where σ_c is the concrete stress at the tendon level due to the initial prestress P_i and the permanent part of the applied load (including self-weight).

A further loss of prestress occurs with time due to relaxation of the tendons (resulting from tensile creep in the highly stressed steel). It is reasonable to assume that for low relaxation strands, the loss of prestress due to relaxation is between 2.5 and 3% of the initial prestress.

13. ANCHORAGE ZONES

The anchorage zone is the zone between the loaded face of the beam and the cross-section at which a linear distribution of stress due to prestress is achieved. For post-tensioned members, the prestress is applied through anchorage or bearing plates at the loaded face. In the case of pretensioned members, the prestress is applied more gradually due to bond between the tendon and the concrete over a distance along the pretensioned tendon known as the *transmission length,* ℓ_t.

The transmission length is considerably shorter in RPC beams than in conventional concrete beams because the bond conditions between the tendons and the RPC containing steel fibres are more favourable. For *Ductal* beams, the transmission length of strand is in the range $20d_b$ to $40d_b$, where d_b is the diameter of the pretensioned strand. When designing the anchorage zone, it is recommended that the lower end of this range be selected as the length over which the concentrated prestressing force is transferred to the concrete. This is conservative and will result in the largest transverse tension within the anchorage zone. However, when checking the stresses on a cross-section near to the end of a beam or when checking the shear strength of such a section, it is conservative to adopt a transmission length closer to the upper end of the range.

For the analysis and design of the anchorage zone, it is sufficient to adopt a strut and tie model which appropriately identifies the primary flow of forces in the anchorage zone (Marti and Rogowski, 1991). If primary tension tie forces are to be resisted by the *Ductal* without the assistance of transverse reinforcement, it is recommended that the dimensions of the section be selected such that the average tensile stress in the RPC tie should not exceed 5.0 MPa and the maximum tensile stress in the RPC should not exceed 8.0 MPa.

Some typical strut and tie models that may be used in anchorage zone design are shown in Figure 13. The internal forces are obtained readily using the principles of statics.

In the case of the concentrically placed tendons of Figure 13a, the average tensile stress in concrete resisting the tension force T_s may be taken as $\sigma_{av} = T_s /(b_w \ell_{TS})$, where b_w is the width of the tie, and may be taken as the effective width of the concrete web at the level of the tendon, and ℓ_{TS} is the tie dimension in the direction of the tendon and may be taken as $30d_b$ or 0.3D, whichever is the greater. For the case of the eccentric tendon in Figure 13b, the tension tie force T_s is resisted by a triangular distribution of transverse tensile stresses, with the maximum transverse tensile stress occurring at the end face of the beam and given by $\sigma_{max} = T_s /(0.5 b_w \ell_{TS})$.

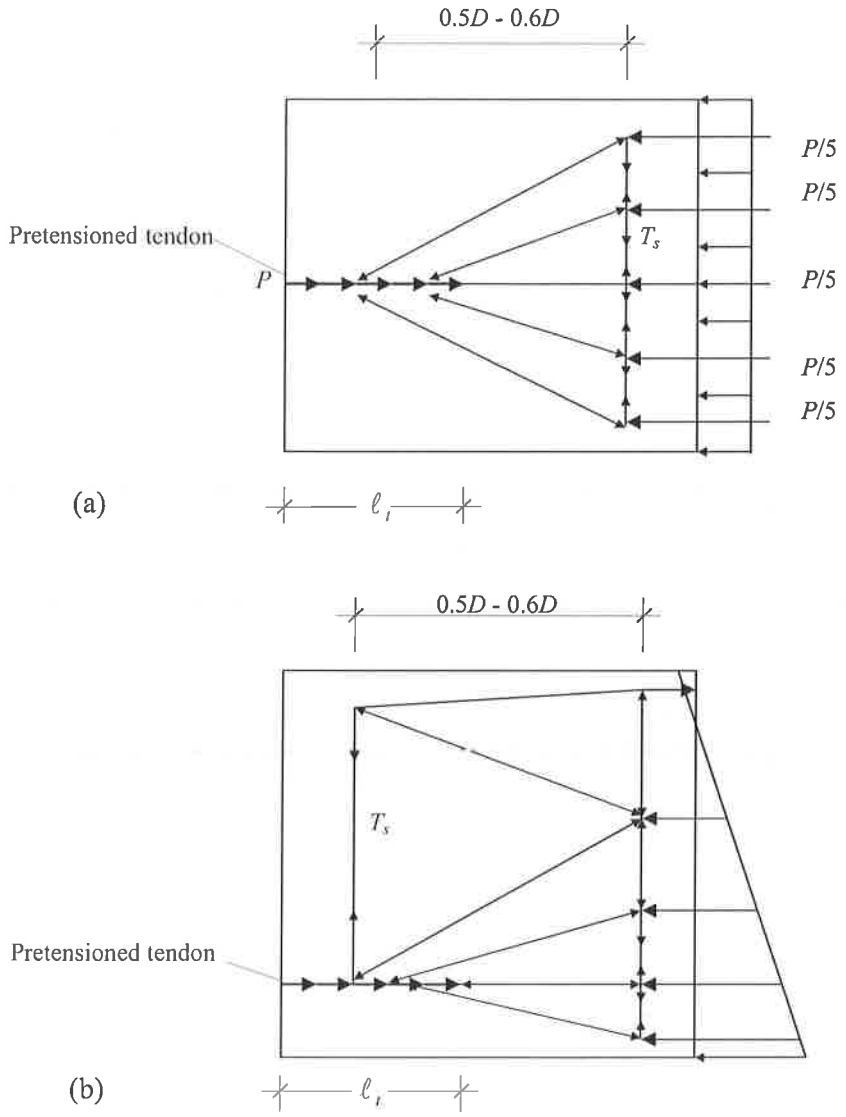

Figure 13 Typical strut and tie models for the anchorage zone

14. REFERENCES

1. AS3600 – 1994, Australian Standard for "Concrete Structures".
2. AS3600 Supp 1 – 1994, Concrete Structures – Commentary.
3. Behloul Mouloud (1996), Analyse et Modelisation du Comportement d'un Matrice Cimentaire Fibree a Ultra Hautes Performances (Betons de Poudres Reactives), France, 180 pp.
4. Behloul, M (1999), Design Rules for DUCTAL Prestressed Beams, 19pp.
5. Chauvel, Adeline, Jacquemmoz and Birelli, First design rules for RPC beams.
6. Dallaire, E., Aitcin, P.C. and Lachemi, M. (1998), High Performance Powder, Civil Engineering Journal, ASCE, pp 48-51.
7. Gilbert and Mickleborough (1990), Design of Prestressed Concrete, Unwin Hyman (London), 504 pp.
8. Gowripalan, Dumitru, Smorchevsky, Marks and B'De Souza (1999), Modified reactive powder concrete for prestressed concrete applications, Conc. Ins. Australia Biennial Conference, Sydney.
9. Hassan W (1999), Optimisation of RPC mixes, undergraduate thesis, UNSW.
10. Kahlil, G (1998), Mechanical properties of RPC using readily available materials in Australia, undergraduate thesis, UNSW.
11. Marti P and Rogowski D (1991), Detailing for Post-tensioning, VSL International.
12. Nguyen VQ (1998), RPC subjected to high temperature, undergraduate thesis, UNSW.
13. Parduli F (1999), High temperature effects on RPC, undergraduate thesis, UNSW.
14. Richard and Cheyrezy (1994?), Ductile ultra high strength concrete (200 – 800 MPa)
15. Te Strake, M. (1997), Feasibility of manufacturing reactive powder concrete in Australia, undergraduate thesis, UNSW.

APPENDIX A - TECHNICAL CHARACTERISTICS OF DUCTAL

DUCTAL is a Reactive Powder Concrete containing steel fibres. Its characteristics are summarised below:

1. STRENGTH CHARACTERISTICS:

Compressive strength:	180 - 230 MPa
Flexural strength:	40 - 50 MPa
Elastic modulus (E):	50 - 60 MPa
Total fracture energy:	20000 - 30000 J/m^2
Elastic fracture energy:	20 - 30 J/m^2

2. RHEOLOGY:

Fluid to self-compacting:

Flow (Abrams cone):	50 - 70 cm
Flow (ASTM Shock table):	250 cm

3. DURABILITY:

Chloride ion diffusion (Cl^-):	0.2 x 10^{-12} m^2/s
Carbonation penetration depth:	< 0.5 mm
Freeze/thaw (after 300 cycles):	100 %
Salt-scaling (loss of residue):	< 10 g/m^2
Abrasion(rel. vol. loss index):	1.2

4. OTHER PROPERTIES

Density:	2.45 - 2.55 t/m^3
Entrapped air content:	2 - 4 %
Capillary porosity (>10μm):	< 1 %
Total porosity:	2 - 6 %
Shrinkage:	0.0005
(post heat treatment - 0.00001)	
Creep coefficient:	
Without heat treatment:	1.2 - 1.8
With heat treatment:	0.2 - 0.5

5. BATCHING AND PLACING:

Ductal can be mixed in a normal industrial concrete mixer. The use of a Pre-mix simplifies the batching sequence and shortens the mixing time.

Ductal is adaptable to any placing technique: cast-in-place, pumping, injection, extrusion.

7. CURING:

Normal curing at 20°C produces the following:

24 hrs after initial set:	fc > 100 MPa
at 28 days:	fc > 180 MPa

Thermal treatment of 90°C applied after final set produces 230 MPa in 4 days.

8. MOULDING/COLOUR CHARACTERISTICS:

The fineness of the material and the fluidity of mix ensures a high ability to replicate the micro-texture of the form surface. The colour of the material varies from light grey to black.

9. PRESTRESSING:

Ductal's mechanical properties are further enhanced by prestressing (either pre- or post-tensioning) and the inclusion of bonded tendons. There is no need to include passive reinforcing bars.

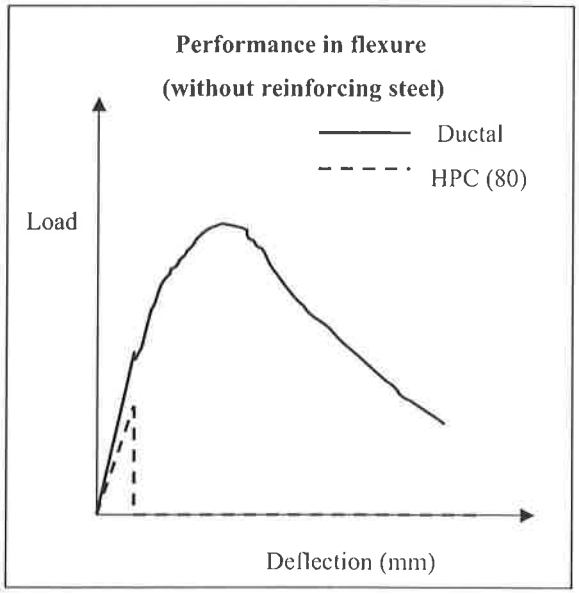

APPENDIX B - FLEXURAL BEHAVIOUR

The moment-curvature relationship for a cross-section may be determined from first principles by enforcing the requirements of strain compatibility, equilibrium and the stress-strain relationships for the materials. The stress-strain relationships adopted here are as follows:

(i) for RPC in compression - Figure 2;

(ii) for RPC in tension - Figure 5; and

(iii) for prestressing steel in tension - an elastic-plastic relationship with an initial elastic modulus of 200000 MPa and a yield stress of 1800 MPa.

Consider the singly-reinforced rectangular cross-section shown in Figure B.1a. The strain distribution when the applied moment is zero is shown in Figure B.1b. When a moment M_i is applied to the cross-section, the strain distribution changes from that in Figure B.1b to that in Figure B.1c. The top fibre strain ε_o and the depth to the neutral axis d_n depend on the magnitude of M.

The stress distribution in the RPC depends on ε_o and d_n, with typical distributions shown in Figure B.1d. The strain in the prestressing steel when $M = 0$ is $\varepsilon_{pe} = P_e/A_pE_p$, where P_e is the effective prestress, A_p is the area of the prestressing steel and E_p is its elastic modulus. The change in strain in the prestressing steel as the moment M_i is applied is equal to the change in strain at the level of the bonded tendon, ie. $|\varepsilon_{ce}| + \varepsilon_{pt}$ (where ε_{ce} and ε_{pt} are defined in Figures B.1b and c, respectively.

To obtain a point on the moment-curvature curve for the cross-section, an appropriate value of ε_o is first selected. A search is then undertaken to determine the value of d_n which satisfies horizontal equilibrium. That is, the sum of the compressive forces on the cross-section (the volume of the compressive stress block) equals the sum of the tensile forces on the cross-section (the volume of the tensile stress block on the RPC plus the tensile force in the prestressing steel, if any). When the correct value of d_n is determined, the moment M corresponding to the current value of ε_o is obtained by taking moments of the compressive and tensile forces on the cross-section about any convenient point. The corresponding curvature is the slope of the strain diagram, $\kappa = \varepsilon_o/d_n$. By incrementing the value of ε_o and repeating the above procedure, the moment-curvature relationship can be readily generated.

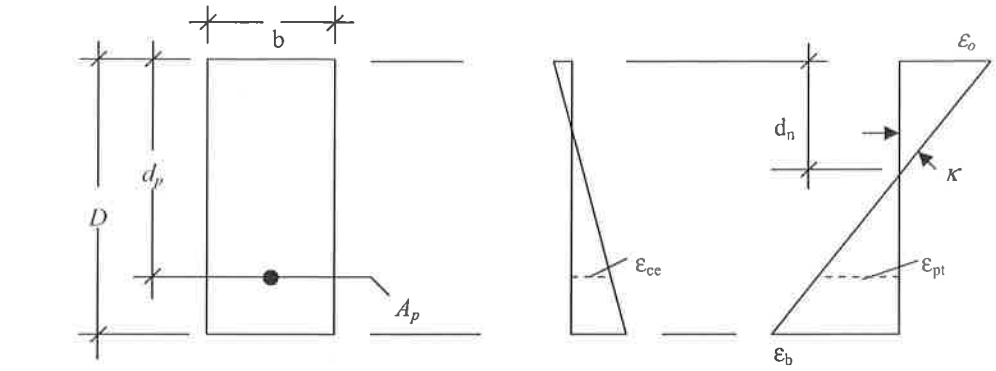

(a) Section (b) Strain (M=0) (c) Strain ($M = M_i$)

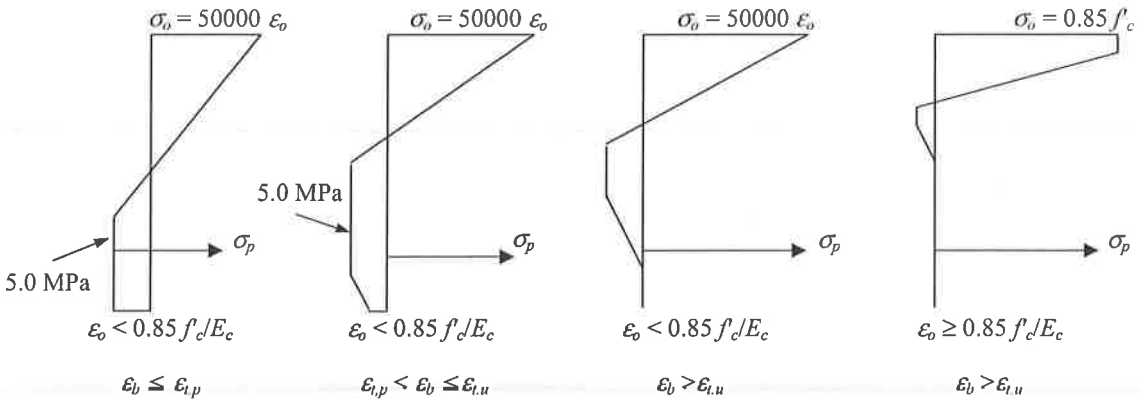

(d) Stress distributions under increasing values of applied moment.

Figure B.1 Stress and strain distributions on a rectangular section in pure bending.

Example B.1 **Non-prestressed, rectangular section**

Data: $b = 200$ mm; $D = 400$ mm; $f'_c = 200$ MPa; $f'_{ct} = 8$ MPa.

Prior to cracking: $I_g = bD^3/12 = 1066.7 \times 10^6$ mm^4; $Z = bD^2/6 = 5.333 \times 10^6$ mm^3. The cracking moment, $M_c = f'_{ct} Z = 42.67$ kNm and the corresponding curvature is $\kappa = M_{cr}/E_c I_g = 0.8 \times 10^{-6}$ mm^{-1} $= \varepsilon_o/d_n = 0.00016 / 200$.

Post-cracking: Values of moment (M), curvature (κ), bottom fibre strain (ε_b), and neutral axis depth (d_n) corresponding to various values of top fibre strain (ε_o) are presented in Table B.1 and the full plot of moment versus curvature is shown in Figure B.2.

Sample calculations:

Sample calculations are provided for the case when the extreme fibre strain $\varepsilon_o = -0.0004$.

- Provided $\varepsilon_b < \varepsilon_{t,p}$ (= 0.004 in this case), the stress distribution is as shown below.

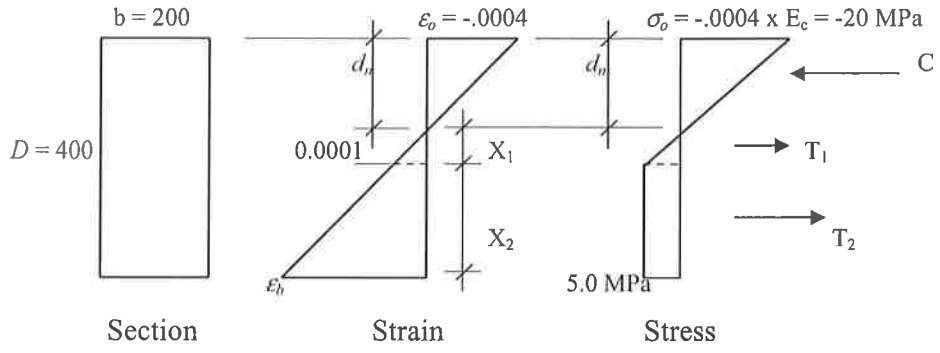

- From strain compatibility,

  $X_1 = .0001.d_n/.0004 = 0.25\ d_n$ and $X_2 = D - 1.25\ d_n$.

- Calculating the volumes of the compressive and tensile stress blocks give

  $C = 0.5\ \sigma_o\ d_n\ b = 0.5 \times -20 \times d_n \times 200 = -2000\ d_n$

  $T_1 = 0.5\ \sigma_b\ X_1\ b = 0.5 \times 5.0 \times 0.25\ d_n \times 200 = 125\ d_n$

  $T_2 = 5.0\ X_2\ b = 5.0 \times (400 - 1.25\ d_n) \times 200 = 400000 - 1250\ d_n$

- Equilibrium requires that

  $C + T_1 + T_2 = 0 \quad \therefore -2000\ d_n + 125\ d_n + 400000 - 1250\ d_n = 0$

  and solving gives $d_n = 128.0$ mm

- Substituting gives: $C = -256000$ N; $T_1 = 16000$ N; $T_2 = 240000$ N; $X_1 = 32$ mm;

  $X_2 = 240$ mm; and $\varepsilon_b = -\varepsilon_o\ (D - d_n)/d_n = 0.00085$ ($< \varepsilon_{t,p}$ $\therefore$ ok)

- The force C is located $d_n/3 = 42.67$ mm below the top fibre.

  The force T_1 is located $(d_n + 2\ X_1/3) = 149.33$ mm below the top fibre.

  The force T_2 is located $(D - X_2/2) = 280.0$ mm below the top fibre.

- Taking moments about the top fibre gives

  $M = T_1\ (d_n + 2\ X_1/3) + T_2\ (D - X_2/2) + C\ d_n/3$

  $= 16000 \times 149.3 + 240000 \times 280 - 256000 \times 42.67 = 58.7 \times 10^6$ Nmm

  $= 58.7$ kNm

- The curvature is: $\kappa = -\varepsilon_o/d_n = 0.0004/128 = 3.125 \times 10^{-6}$ (mm^{-1}).

Table B.1

ε_o x 10^{-6}	d_n (mm)	ε_b x 10^{-6}	M (kNm)	κ x 10^{-6} (mm^{-1})
-186	181.9	223	42.7	1.023
-200	177.8	250	44.4	1.125
-250	163.3	363	49.5	1.531
-300	150.0	500	53.3	2.000
-400	128.0	850	58.7	3.125
-500	111.1	1300	62.2	4.500
-600	98.0	1850	64.8	6.125
-700	87.5	2500	66.7	8.000
-800	79.0	3250	68.2	10.13
-900	72.0	4101	69.3	12.50
-1000	64.9	5163	67.9	15.41
-1100	56.3	6714	61.3	19.53
-1170	46.6	8875	48.1	25.11

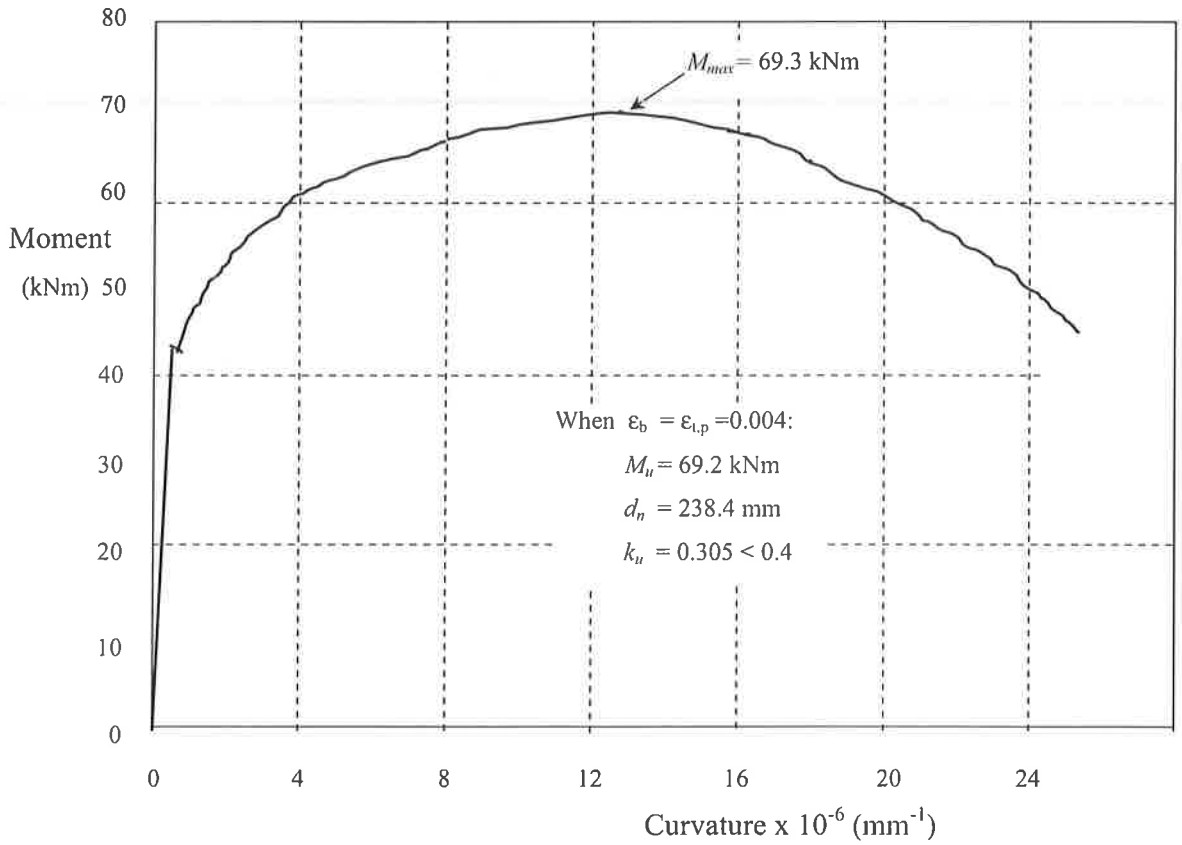

Figure B.2 Moment versus curvature for non-prestressed, unreinforced section.

Example B.2 **Prestressed, rectangular sections (effect of varying A_p)**

Data: $b = 200$ mm; $D = 400$ mm; $d_p = 300$ mm; $f'_c = 200$ MPa; $f'_{cl} = 8$ MPa.

Variables: Four cross-sections to be considered:

(i) $A_p = 250$ mm^2 and $P_e = 315$ kN $(P_e/A_p = 1260$ MPa $= 0.7 f_{pu})$;

(ii) $A_p = 500$ mm^2 and $P_e = 630$ kN $(P_e/A_p = 1260$ MPa $= 0.7 f_{pu})$;

(iii) $A_p = 750$ mm^2 and $P_e = 945$ kN $(P_e/A_p = 1260$ MPa $= 0.7 f_{pu})$; and

(iv) $A_p = 1000$ mm^2 and $P_e = 1260$ kN $(P_e/A_p = 1260$ MPa $= 0.7 f_{pu})$.

Comments: These four sections range from heavily prestressed (Section iv) to lightly prestressed (Section i). The moment and curvature corresponding to various values of top fibre strain are presented in Table B.2 and the moment curvature plots are shown in Figure B.3. Note the decrease in ductility with increasing A_p . Also note that a reasonable estimate of M_u is obtained by taking $\varepsilon_o = -0.0035$.

Sample Calculations:

Sample calculations are provided for the section where $A_p = 500$ mm^2 and $P_e = 630$ kN (Section ii) and when the extreme fibre compressive strain is $\varepsilon_o = -0.0035$. (This is the top fibre strain assumed at the ultimate limit state).

- Provided $\varepsilon_b > \varepsilon_{t,u}$ (= 0.01 in this case), the stress distribution is as shown below. It is assumed initially (and subsequently checked) that the prestressing steel is at yield (ie. $\varepsilon_p > 0.009$). Note that $0.85 f'_c / E_c = 0.0034$

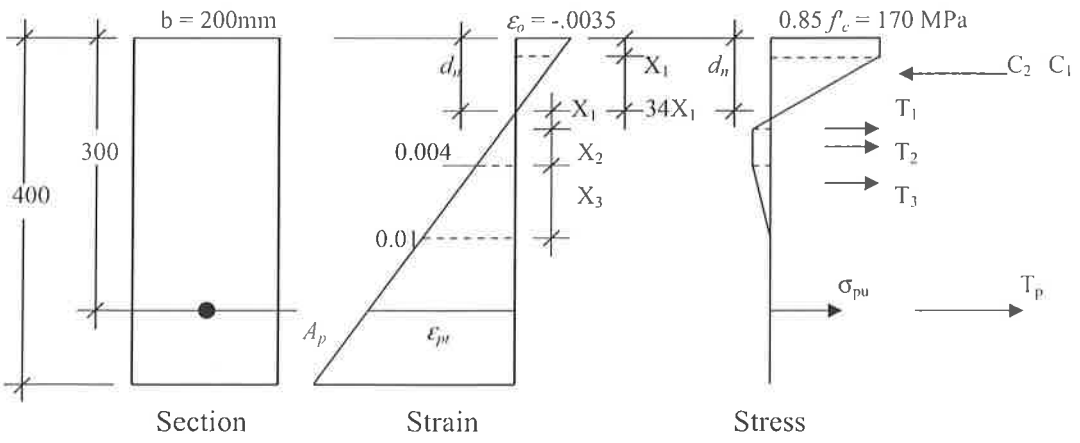

- From strain compatibility,

$X_1 = d_n/35$; $X_2 = 39\, d_n/35$; and $X_3 = 60\, d_n/35$.

- Calculating the volumes of the compressive and tensile stress blocks give

  $C_1 = 0.85 f_c' (d_n/35) b = 170 \times (d_n/35) \times 200 = -971.4\ d_n$

  $C_2 = 0.5 \times 0.85 f_c' (34 d_n/35) b = 0.5 \times 170 \times (34 d_n/35) \times 200 = -16514.3\ d_n$

  $T_1 = 0.5 \times 5.0\ X_1\ b = 0.5 \times 5.0 \times (d_n/35) \times 200 = 14.3\ d_n$

  $T_2 = 5.0\ X_2\ b = 5.0 \times (39 d_n/35) \times 200 = 1114.3\ d_n$

  $T_3 = 0.5 \times 5.0\ X_3\ b = 0.5 \times 5.0 \times (60 d_n/35) \times 200 = 857.1\ d_n$

  $T_p = A_p f_{pu} = 500 \times 1800 = 900\ 000$ N

- Equilibrium requires that

  $C_1 + C_2 + T_1 + T_2 + T3 + T_p = 0$

  $\therefore (-971.4 - 16514.3 + 14.3 + 1114.3 + 857.1)\ d_n + 900000 = 0$

  and solving gives $d_n = 58.07$ mm

- Substituting gives: $C_1 = -56406$ N; $C_2 = -958894$; $T_1 = 830$ N; $T_2 = 64701$ N; $T_3 = 49769$; $T_p = 900000$ N; $X_1 = 1.659$ mm; $X_2 = 64.70$ mm; and $X_3 = 99.539$ mm.

  Also $\varepsilon_{pt} = .0035(300-58.07)/58.07 = 0.0146$ and so $\varepsilon_p >> \varepsilon_p = 0.009$.

  In addition, $\varepsilon_b = .0035\ (D - d_n)/d_n = 0.0206 >> 0.01$

  $\therefore$ The initial assumption are satisfied.

- Taking moments about the top fibre gives

  $$M = T_1 (d_n + 2 X_1/3) + T_2 (d_n + X_1 + X_2/2) + T_3 (d_n + X_1 + X_2 + X_3/3)$$
  $$T_p d_p + C_1 X_1/2 + C_2 (X_1 + 34X_1/3)$$
  $$= 264.2 \text{ kNm}$$

- The curvature is: $\kappa = -\varepsilon_o/d_n = 0.0035/58.07 = 60.28 \times 10^{-6}$ (mm^{-1}).

Table B.2

A_p = 250 mm^2 and P_e = 315 kN						A_p = 500 mm^2 and P_e = 630 kN					
ε_o x 10^{-6}	d_n (mm)	ε_b x 10^{-6}	ε_p	M kNm	κ x 10^{-6} mm^{-1}	ε_o x 10^{-6}	d_n (mm)	ε_b x 10^{-6}	ε_p	M kNm	κ x 10^{-6} mm^{-1}
39.4		-197	.0063	0	-0.591	78.8		-394	.0063	0	-1.181
-322	267.2	160	.0065	96.64*	1.205	-489	301.3	160	.0066	152.2*	1.622
-350	250.7	208	.0065	99.70	1.396	-500	294.1	180	.0066	153.1	1.700
-500	203.8	481	.0067	120.3	2.453	-600	261.2	319	.0067	171.6	2.297
-750	157.0	1161	.0071	142.0	4.778	-800	215.1	687	.0069	198.9	3.719
-1000	130.1	2074	.0077	158.6	7.686	-1000	185.1	1161	.0072	219.9	5.403
-1250	113.2	3168	.0085	173.9	11.05	-1250	160.1	1874	.0077	242.8	7.809
-1400	105.8	3894	.0090	182.9	13.24	-1500	143.2	2690	.0082	264.4	10.48
-1450	102.6	4205	.0092	178.4	14.14	-1750	131.2	3586	.0088	285.5	13.34
-1500	99.42	4535	.0095	172.0	15.09	-1850	126.5	4000	.0091	292.2	14.62
-1750	84.24	6560	.0109	157.2	20.78	-2000	117.6	4801	.0097	280.0	17.00
-2000	68.90	9611	.0131	162.6	29.03	-2250	104.1	6393	.0108	272.7	21.61
-2250	55.14	14072	.0160	148.6	40.81	-2500	91.78	8396	.0123	276.3	27.24
-2500	46.30	19100	.0201	140.9	54.00	-2750	80.20	10960	.0141	278.9	34.29
-3000	35.48	30822	.0288	135.3	84.55	-3000	70.96	13910	.0160	271.0	42.28
-3400	30.09	41801	.0369	133.8	113.0	-3500	58.07	20600	.0210	264.2	60.28
-3500	29.03	44700	.0391	133.6	120.6	-4000	50.53	27700	.0260	261.6	79.17
-4000	25.26	59300	.0499	132.9	158.3	-5000	45.19	39300	.0350	258.7	110.6
						-7000	51.53	47300	.0403	250.0	135.8
A_p = 750 mm^2 and P_e = 945 kN						A_p = 1000 mm^2 and P_e = 1260 kN					
ε_o x 10^{-6}	d_n (mm)	ε_b x 10^{-6}	ε_p	M kNm	κ x 10^{-6} mm^{-1}	ε_o x 10^{-6}	d_n (mm)	ε_b x 10^{-6}	ε_p	M kNm	κ x 10^{-6} mm^{-1}
118.1		-591	.0063	0	-1.772	157.5		-788	.0063	0	-2.36
-660	322.0	160	.0067	209.4*	2.05	-836*	335.8	160	.0067	268.1*	2.49
-750	292.7	274	.0067	227.1	2.56	-850	330.5	179	.0068	270.3	2.57
-1000	238.9	674	.0069	267.0	4.19	-1000	293.4	364	.0069	301.5	3.41
-1250	204.9	1190	.0073	298.0	6.10	-1250	249.7	752	.0071	342.5	5.01
-1500	182.0	1797	.0077	325.4	8.24	-1500	220.2	1225	.0074	376.6	6.81
-1750	165.7	2476	.0081	351.4	10.56	-2000	183.6	2358	.0081	437.1	10.90
-2000	153.6	3210	.0086	376.9	13.02	-2250	171.7	2993	.0085	466.1	13.11
-2200	145.6	3846	.0091	396.2	15.11	-2500	162.3	3661	.0090	494.9	15.40
-2300	139.7	4284	.0094	400.0	16.46	-2600	156.9	4027	.0092	499.8	16.57
-2400	134.2	4754	.0097	388.6	17.88	-2800	146.3	4857	.0098	493.3	19.14
-2500	128.9	5256	.0100	385.7	19.39	-3000	136.6	5785	.0104	492.0	21.96
-2750	116.8	6669	.0110	384.7	23.55	-3400	119.6	7976	.0120	499.7	28.44
-3000	105.8	8342	.0120	390.2	28.34	-3500	115.8	8592	.0124	503.1	30.23
-3400	90.27	11670	.0146	393.8	37.67	-3750	107.6	10194	.0136	510.6	34.86
-3500	87.10	12574	.0153	391.9	40.19	-4000	101.1	11833	.0147	506.5	39.58
-4000	75.79	17111	.0185	386.2	52.78	-4500	93.28	14796	.0168	500.4	48.24
-6000	69.48	28540	.0266	371.8	86.36	-5000	90.37	17130	.0185	494.6	55.32
-7000	77.30	29250		360.1	90.56	-7000	103.1	20167	.0202	460.2	67.90

* The cracking moment applied to the uncracked cross-section.

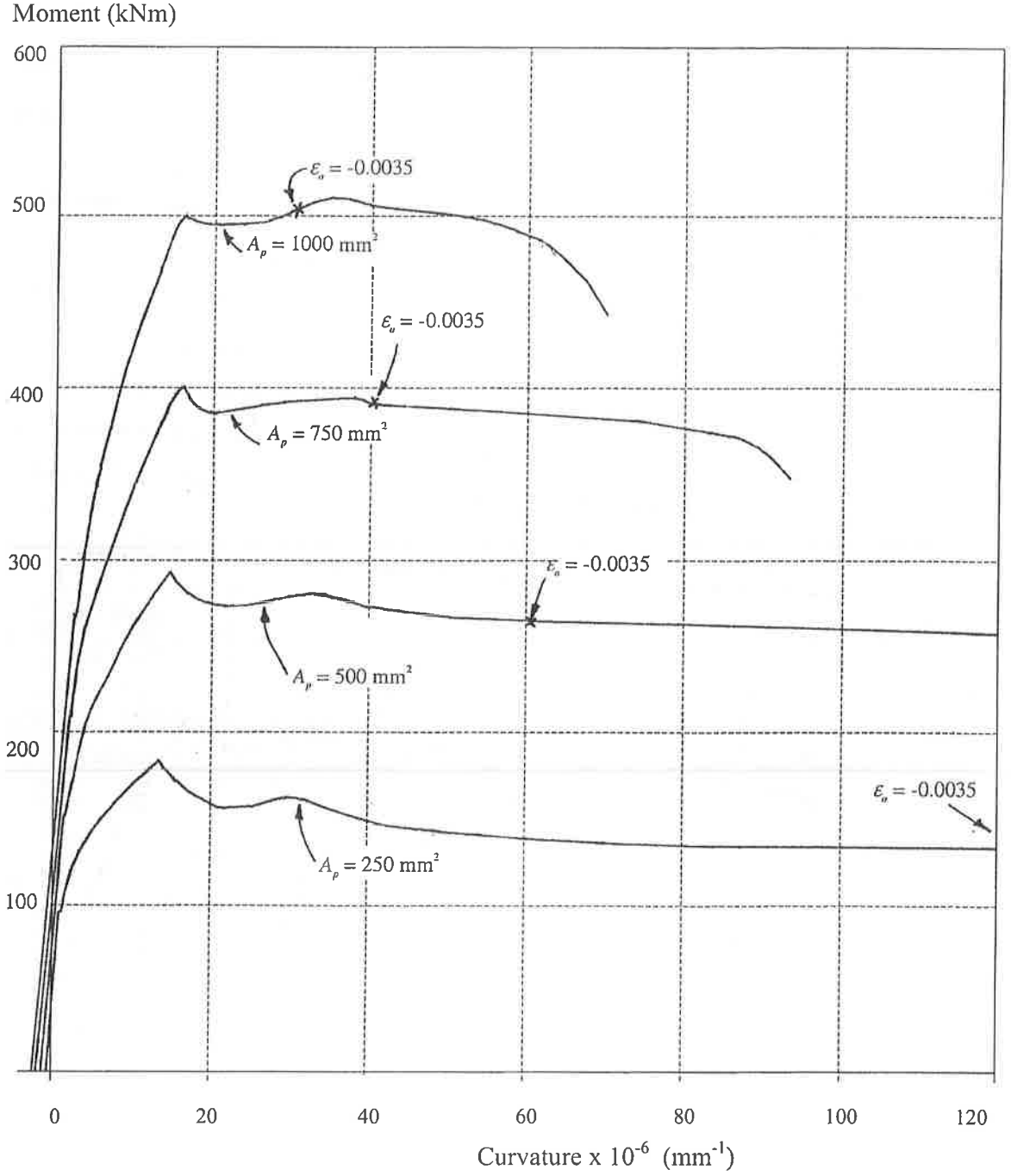

Figure B.3 Moment versus curvature for prestressed, rectangular sections

Example B.3 **Prestressed, rectangular sections (effect of varying P_e)**

Data: b = 200 mm; D = 400 mm; d_p = 300 mm; f_c' = 200 MPa; f_{ct}' = 8 MPa; A_p = 750 mm^2. Three levels of prestressing force are considered: P_i = 0 , 472.5 kN and 945 kN

Comments: When P_i = 0 , the section is reinforced with unstressed tendons. When P_i = 945 kN, the section is fully-prestressed with an initial prestress of 0.7 f_{pu}. The moment and curvature corresponding to various values of top fibre strain are presented in Table B.3 and the moment curvature plots are shown in Figure B.4.

Note that the level of prestress has little effect on the ultimate strength of the section, but a very significant effect on the cracking moment and the post-cracking stiffness of the section, ie. a very significant effect on the behaviour under service loads.

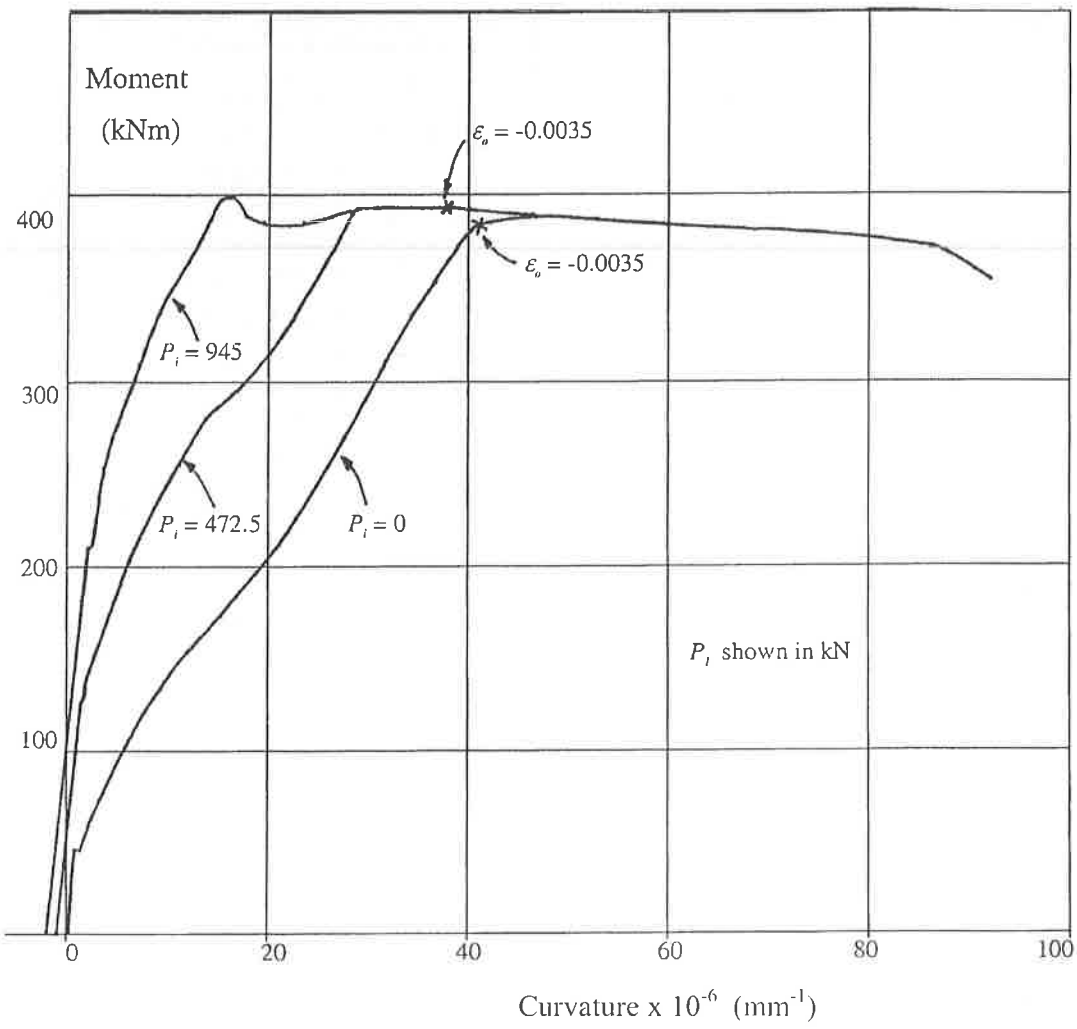

Figure B.4 Moment versus curvature for prestressed, rectangular sections

Table B.3

$A_p = 750$ mm^2 and $P_i = 0$ kN					
ε_u x 10^{-6}	d_n (mm)	ε_b x 10^{-6}	ε_p	M kNm	κ x 10^{-6} mm^{-1}
-166	203.6	160	.00008	44.63*	0.815
-200	186.0	230	.00012	46.62	1.076
-500	136.8	969	.0006	80.36	3.670
-1000	109.4	2658	.0017	131.9	9.145
-1500	99.69	4519	.0030	172.9	15.05
-2000	93.82	6527	.0044	211.5	21.30
-2500	89.77	8639	.0059	271.5	27.85
-2800	87.94	9937	.0067	312.0	31.84
-3500	85.28	12916	.0088	384.0	41.04
-3750	80.68	14843	.0102	388.5	46.48
-4000	75.79	17111	.0118	386.2	52.78
-5000	67.78	24506	.0171	379.5	73.77
-6000	69.48	28543	.0199	371.8	86.36
-7000	77.30	29223	.0201	360.1	90.56

$A_p = 750$ mm^2 and $P_i = 472.5$ kN					
ε_u x 10^{-6}	d_n (mm)	ε_b x 10^{-6}	ε_p	M kNm	κ x 10^{-6} mm^{-1}
59		-295	.00315	0	-0.886
-413	288.3	160		127.0*	1.433
-500	254.7	285	.00345	141.7	1.963
-1000	168.7	1372	.00414	203.0	5.93
-1500	137.2	2874	.00514	254.1	10.94
-1750	128.3	3705	.00570	279.7	13.64
-2000	121.7	4575	.0063	293.1	16.44
-2500	111.9	6441	.0076	331.2	22.35
-3000	105.0	8428	.0089	387.9	28.57
-3400	90.27	11667	.0112	393.8	37.67
-3500	87.10	12574	.0119	391.8	40.19
-4000	75.79	17111	.0152	386.1	52.78
-5000	67.78	24506	.0205	379.5	73.77
-6000	69.48	28543	.0233	371.8	86.36

$A_p = 750$ mm^2 and $P_i = 945$ kN					
ε_u x 10^{-6}	d_n (mm)	ε_b x 10^{-6}	ε_p	M kNm	κ x 10^{-6} mm^{-1}
118.1		-591	.0063	0	-1.772
-660	322.0	160	.0067	209.4*	2.05
-750	292.7	274	.0067	227.1	2.56
-1000	238.9	674	.0069	267.0	4.19
-1250	204.9	1190	.0073	298.0	6.10
-1500	182.0	1797	.0077	325.4	8.24
-1750	165.7	2476	.0081	351.4	10.56
-2000	153.6	3210	.0086	376.9	13.02
-2200	145.6	3846	.0091	396.2	15.11
-2300	139.7	4284	.0094	400.0	16.46
-2400	134.2	4754	.0097	388.6	17.88
-2500	128.9	5256	.0100	385.7	19.39
-2750	116.8	6669	.0110	384.7	23.55
-3000	105.8	8342	.0120	390.2	28.34
-3400	90.27	11670	.0146	393.8	37.67
-3500	87.10	12574	.0153	391.9	40.19
-4000	75.79	17111	.0185	386.2	52.78
-6000	69.48	28540	.0266	371.8	86.36
-7000	77.30	29250		360.1	90.56

* The cracking moment applied to the uncracked cross-section.

APPENDIX C - DESIGN CALCULATIONS

EXAMPLE C.1

Simply-supported box girder bridge spanning 35 m and designed to carry a HLP loading spread over two traffic lanes. Each girder is 2.4 m wide and carries 65% of the load from a single traffic lane.

1. Traffic Loading: HLP Loading (over two lanes):

Design moments due to traffic load at midspan:

SLS = 0.5 x 1.1 x 0.65x 17200 = 6150 kNm

ULS = 1.5 x 6150 = 9225 kNm

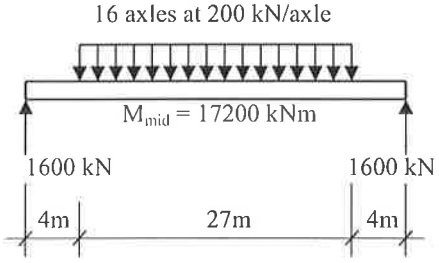

2. Material properties:

At transfer: f'_{cp} = 100 MPa; E_{cp} = 40000 MPa; and f'_{cf} = 5 MPa.

After 28 days: f'_c = 180 MPa; E_c = 50000 MPa; and f'_{cf} = 8 MPa.

For long-term analysis take ϕ^* = 1.2 and ε_{sh}^* = -0.0005.

1/12.7 mm dia strand = 100 mm^2; 1/15.2 mm dia strand = 143 mm^2; f_{pu} = 1820 MPa.

3. Cross-section:

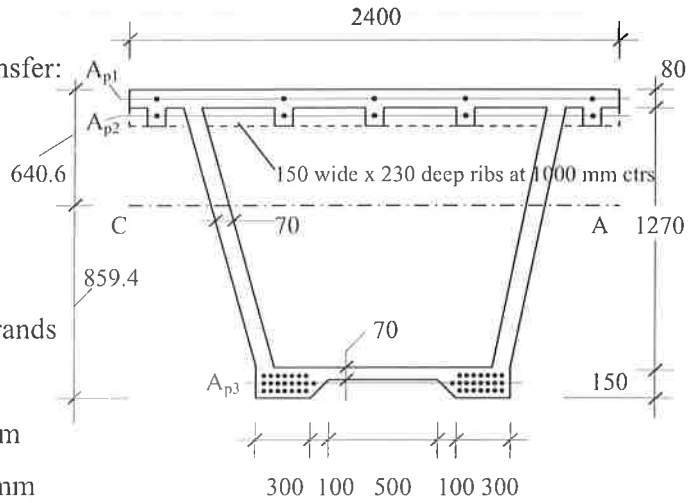

Transformed properties at transfer:

A = 605970 mm^2;

I = 213170 x 10^6 mm^4;

Z_t = 332.8 x 10^6 mm^3;

Z_b = 248.0 x 10^6 mm^3;

$A_{p1} = A_{p2}$ = 5/12.7 mm dia strands

= 5 x 100 = 500 mm^2;

d_{p1} = 35 mm ; e_{p1} = -605.6 mm

d_{p2} = 165 mm ; e_{p2} = -475.6 mm

$P_{i1} = P_{i2}$ = 5 x 137 = 685 kN;

A_{p3} = 44/15.2 mm dia strands

= 44 x 143 = 6292 mm^2;

d_{p3} = 1425 mm ; e_{p3} = 784.4 mm;

P_{i3} = 44 x 196 = 8624 kN.

Initial prestress/strand after transfer (assuming 6% elastic shortening losses) for 12.7 & 15.2 mm dia , respectively:

P_i = 100 x 0.8 x 1820 x 0.94 = 137 kN

P_i = 143 x 0.8 x 1820 x 0.94 = 196 kN.

Self-weight of girder = 14.71 kN/m.

4. Extreme fibre stresses at transfer:

$P_{i1} = P_{i2} = 685$ kN; $e_{p1} = -605.6$ mm; $e_{p2} = -475.6$ mm; $P_{i3} = 8624$ kN; $e_{p3} = 784.4$ mm.

At support:

$$\sigma_{top} = -\frac{(685+685+8624)\times 10^3}{6059700} + \frac{(685(-605.6-475.6)+8624\times 784.4)\times 10^3}{332.8\times 10^6}$$

$$= -16.49 + 18.10 = +1.61\,\text{MPa}$$

$$\sigma_{bot} = -\frac{(685+685+8624)\times 10^3}{605970} - \frac{(685(-605.6-475.6)+8624\times 784.4)\times 10^3}{248.0\times 10^6}$$

$$= -16.49 - 24.29 = -40.78\,\text{MPa}$$

At midspan:

Moment due to self-weight = 14.71 x $35^2/8$ = 2252 kNm

$$\sigma_{top} = +4.41 - \frac{2252\times 10^6}{332.8\times 10^6} = -5.16\,\text{MPa}$$

$$\sigma_{bot} = -40.78 + \frac{2252\times 10^6}{248.0\times 10^6} = -31.70\,\text{MPa.}$$

Note that the maximum compressive stress at transfer is less than $0.6\,f'_{cp} = 60$ MPa and the maximum tensile stress is less than 5 MPa.

5. Deflection at transfer:

The curvature at the supports (κ_s) and at midspan (κ_m) immediately after transfer are

$$\kappa_s = \frac{-(\sigma_{top}-\sigma_{bot})}{E_c D} = \frac{-(1.61+40.78)}{40000\times 1500} = -0.707\times 10^{-6}\,\text{mm}^{-1}$$

$$\kappa_m = \frac{-(\sigma_{top}-\sigma_{bot})}{E_c D} = \frac{-(-5.16+31.70)}{40000\times 1500} = -0.442\times 10^{-6}\,\text{mm}^{-1}$$

and the deflection at midspan is

$$\Delta = \frac{35000^2}{96}(-0.707+10\times -0.442-0.707) = -74.4\,\text{mm}\ (\uparrow)$$

6. Long-term analysis under sustained loads:

- The sustained load is taken to be self-weight + 3.0 kN/m = 17.71 kN/m.
- The moment at midspan due to sustained load is M_{sus}= 17.71 x $35^2/8$= 2712 kNm.

- The age-adjusted effective modulus method is used to determine time-dependent behaviour. Taking E_c = 40000 MPa (as most of the sustained load is applied at transfer, ie. prestress and self-weight), ϕ^* = 1.2, χ = 0.8, ε_{sh}^* = -0.0005 and 2.5%

relaxation in the strand, the instantaneous and final stresses and strains at the sections at midspan and at the supports are shown below.

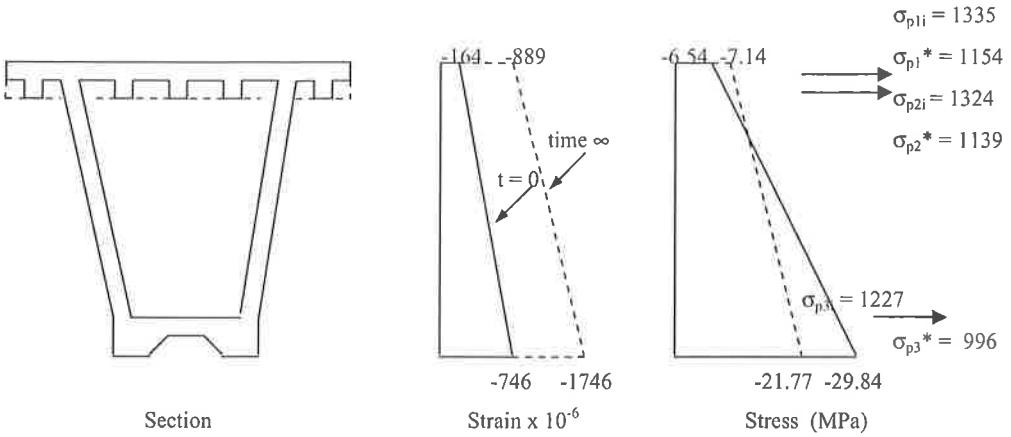

At t = 0: $\kappa_i = -0.388 \times 10^{-6}$ mm^{-1}

At time ∞: $\kappa = -0.571 \times 10^{-6}$ mm^{-1}

Section at midspan

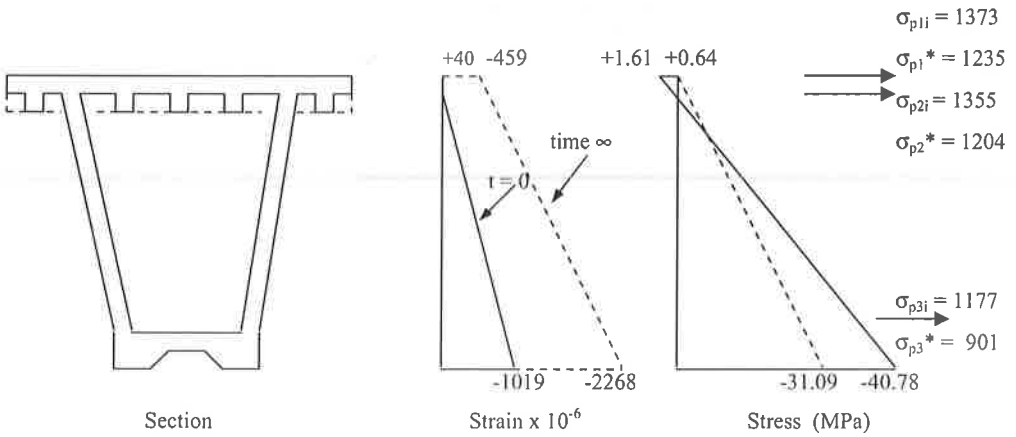

At t = 0: $\kappa_i = -0.706 \times 10^{-6}$ mm^{-1}

At time ∞: $\kappa = -1.206 \times 10^{-6}$ mm^{-1}

Section at support

7. Final deflection under sustained loads:

The final deflection at midspan under the sustained load after creep and shrinkage is

$$\Delta = \frac{35000^2}{96}(-1.21 + 10 \times -0.571 - 1.21) = -103.7\,\text{mm} \quad (\uparrow)$$

Note: From a time analysis, the final curvature at the support is -1.21×10^{-6} mm^{-1}.

As calculated at step5, the deflection at midspan immediately after transfer is 74.4 mm(↑). This upward deflection decreases when the additional superimposed dead load is

applied and then gradually increases with time to a final value of 103.7 mm (↑). Any traffic load will reduce this upward camber.

8. Losses of prestress at midspan:

From the results of the time analysis presented in Step 6:

Prior to transfer: $\sigma_{p1} = \sigma_{p2} = \sigma_{p3} = 1371$ MPa.

After transfer: $\sigma_{p1} = 1335$ MPa (2.6% immediate losses)

$\sigma_{p2} = 1324$ MPa. (3.4% immediate losses)

$\sigma_{p3} = 1227$ MPa. (10.5% immediate losses)

After time-dependent losses: $\sigma_{p1} = 1154$ MPa (15.8% total losses) and

$\sigma_{p2} = 1139$ MPa (16.9% total losses)

$\sigma_{p3} = 996$ MPa (27.4% total losses).

9. Stresses (after all losses) and deflection due full traffic load:

Midspan moment due to HLP loading (serviceability limit state) is M = 6150 kNm.

Extreme fibre stresses at midspan:

$$\sigma_{top} = -7.14 - \frac{6150\times10^6}{332.8\times10^6} = -25.62\,\text{MPa}$$

$$\sigma_{bot} = -21.77 + \frac{6150\times10^6}{248.0\times10^6} = +3.03\,\text{MPa} \qquad < f'_{cf}\ (= 8\ \text{MPa}).$$

Cracking is not likely under full service loads.

The curvature at midspan caused by the HLP loading is therefore

$$\kappa = \frac{M}{E_c I} = \frac{6150\times10^6}{50000\times213170\times10^6} = 0.577\times10^{-6}\,\text{mm}^{-1}$$

and the corresponding instantaneous deflection is

$$\Delta = \frac{35000^2}{9.6}\times0.577\times10^{-6} = 73.6\,\text{mm} \quad (\downarrow) = \text{Span}/475.$$

The nett midspan deflection under the full in-service HLP loading after all losses is upward and equal to -103.7 + 73.6 = -30.1 mm (↑).

10. Flexural strength (ultimate limit state):

For D = 1500 mm, $\varepsilon_{t,p} = 0.0015$ and $\varepsilon_{t,u} = 0.007$. By equating the compressive and tensile forces of the cross-section at ultimate, the value of d_n is found to be 62.97 mm.

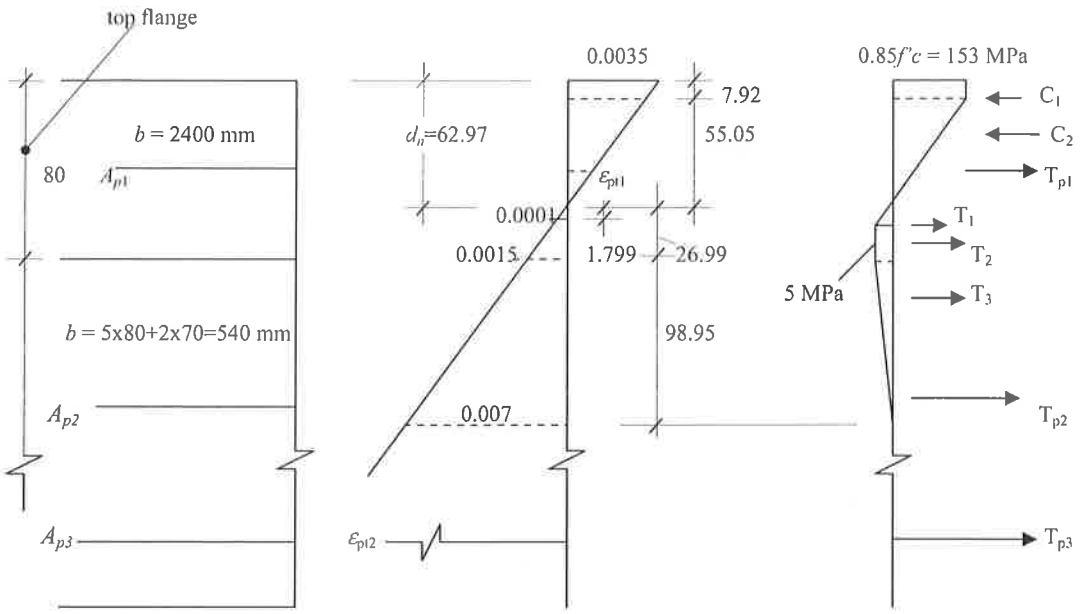

For horizontal equilibrium, the value of d_n is 62.97 mm and therefore

$C_1 = 7.92 \times 153 \times 2400 \times 10^{-3}$ = 2907 kN

$C_2 = 0.5 \times 55.05 \times 153 \times 2400 \times 10^{-3}$ = 10107 kN

ΣC = 13014 kN

$T_1 = 0.5 \times 5.0 \times 1.799 \times 2400 \times 10^{-3}$ = 11 kN

$T_2 = 5.0 \times 15.23 \times 2400 \times 10^{-3} + 5.0 \times 9.95 \times 540 \times 10^{-3}$ = 210 kN

$T_3 = 0.5 \times 5.0 \times 98.95 \times 540 \times 10^{-3}$ = 134 kN

$\varepsilon_{p1} = -0.0035 \times (62.97-35)/62.97 = -0.001555$; $\varepsilon_{ce} = -7.48/50000 = -0.000150$;

$\varepsilon_{pe} = \sigma_{pe}/E_p = 1154/2\text{x}10^5 = 0.005770$

$\therefore \varepsilon_{p1} = .005770 - .001555 + .000150 = 0.004365$ and $\sigma_{p1} = \varepsilon_{p1} E_p = 873$ MPa.

$\varepsilon_{p2} >> \varepsilon_{py}$ (= 0.009) and hence $\sigma_{p2} = f_{py} = 1800$ MPa. Therefore,

$T_{p1} = 500 \times 870 \times 10^{-3}$ = 437 kN

$T_{p2} = 500 \times 1800 \times 10^{-3}$ = 900 kN

$T_{p2} = 6292 \times 1800 \times 10^{-3}$ = 11326 kN

ΣT = 13018 kN $\approx \Sigma C$ $\therefore$ ok

Taking moments of these internal forces about the top fibre gives the ultimate strength of the section:

$$M_u = [11326 \times 1425 + 900 \times 165 + 437 \times 35 + 11 \times 64.17 + 210 \times 74.0 + 134 \times 122.9 - 2907 \times 3.96 - 10107 \times 26.27] \times 10^{-3}$$

$$= 16050 \text{ kNm}$$

and the *design ultimate moment* is $\phi M_u = 0.8 \times 16050 = 12840$ kNm.

The *design moment* for the strength limit state is

$$M^* = 1.25 \times 2712 + 9225 = 12615 \text{ kNm} \quad < \phi M_u$$

Therefore, the section has adequate flexural strength and since $d_n << 0.4d$ the section is ductile. In this case, the resultant of the tensile forces located in the tension zone (ie. the resultant of T_1 ,T_2, T_3, T_{p2} and T_{p3}) is located at $d = 1295$ mm below the top fibre.

11. Shear strength (ultimate limit state):

The *design ultimate shear force* is taken to be the maximum shear force (factored for the strength limit state) at a section $d = 1295$ mm from the support. Consider the following factored load case:

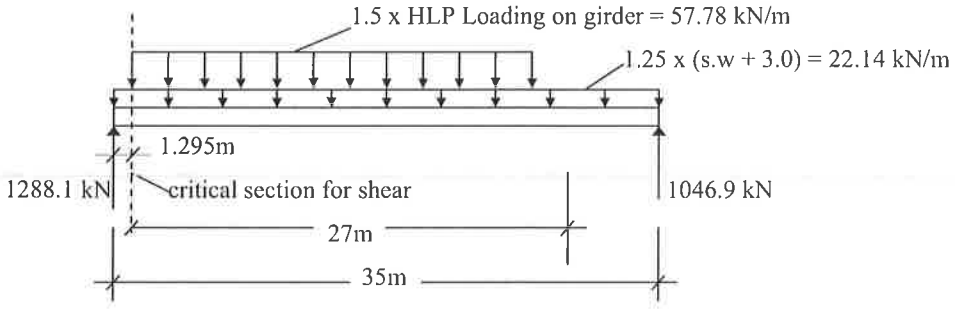

At the critical section for shear, $V^* = 1259$ kN (and the bending moment is 1650 kNm).

At the centroidal axis of the uncracked section:

$$Q = 2400 \times 80 \times 600.6 + 150 \times 400 \times 485.6 + 0.5 \times 560.6^2 \times 140$$
$$+ 2000\,(605.6 + 475.6) = 168.6 \times 10^6 \text{ mm}^3;$$

$b = 140$ mm; $I = 213170 \times 10^6$ mm^4 and the shear stress caused by V^* is

$$\tau = \frac{V^* Q}{I\ b} = \frac{1259 \times 10^3 \times 168.6 \times 10^6}{213170 \times 10^6 \times 140} = 7.11 \text{ MPa}$$

From the final stress distribution after all losses at the section at the support (plotted in Step 6), the effective prestressing force at each steel level after all losses are

$$P_{e1} = 1235 \times 500 = 618 \text{ kN};\ P_{e2} = 1204 \times 500 = 602 \text{ kN};\ P_{e3} = 901 \times 6292 = 5669 \text{ kN}$$

and the normal stress at the centroidal axis is $\sigma = -13.55$ MPa.

Equation (7.3) gives

$$\sigma_1 = \frac{-13.55}{2} + \sqrt{(\frac{-13.55}{2})^2 + 7.11^2} = +3.05\,\text{MPa} < 5.0+0.13\sqrt{f_c'}\ (= 6.74\ \text{MPa})$$

In the web just below the top flange:

$Q = 2400 \times 80 \times 600.6 + 2000 \times 605.6 = 116.5 \times 10^6\ \text{mm}^3$

and the shear stress caused by V^* is

$$\tau = \frac{1259\times10^3 \times 116.5\times10^6}{213170\times10^6 \times 140} = 4.92\ \text{MPa}.$$

The normal stress is obtained from the final stress distribution after all losses at the support (plotted in Step 6) and is equal to

$\sigma = -1.05$ MPa.

From Equation (7.3),

$$\sigma_1 = \frac{-1.05}{2} + \sqrt{(\frac{-1.05}{2})^2 + 4.92^2} = +4.42\,\text{MPa} < 5.0+0.13\sqrt{f_c'}\ (= 6.74\ \text{MPa}).$$

Hence, the girder satisfies the shear strength design requirements.

12. Design of Deck:

Loads:

Dead load:	50mm bitumen seal	=	1.0 kPa
	Self-weight: 80mm slab	=	2.0 kPa
	150 x 80mm rib	=	0.30 kN/m
	150 x 140mm rib	=	0.53 kN/m
Wheel load:	W7 (on 500mmx200mm area)	=	70.0 kN
	Dynamic allowance (25%)	=	17.5 kN
	Total wheel load	=	87.5 kN

Deck Layout:

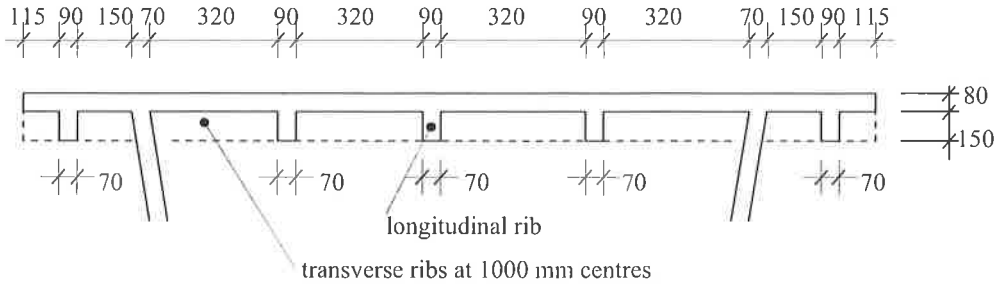

Slab between longitudinal ribs:

- Clear span = 320 mm; slab thickness = 80mm.
- **Ultimate flexural strength:** For an unreinforced section 1000mm wide and 80mm deep, M_u occurs when the bottom fibre strain is $\varepsilon_{b,u} = \varepsilon_{t,p} = 0.0004$ (see Section 5.1 (Figure 9) and also Example B.1) and is calculated to be M_u = 13.84 kNm/m, with d_n = 14.55 mm and d = 47.7 mm.
- **Design for W7 wheel load** (i) with 500 mm dimension of the contact area in the direction of the span; and (ii) with 200 mm dimension of the contact area in the direction of the span.

(i) Moment resisting width of Slab = 200 + 244 = 444 mm*.

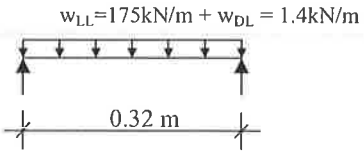

Maximum working moment (SLS):

M_{max} = 80% of simply-supported clear span moment

= 0.8 (M_{DL} + M_{LL}) = 0.8 (0.02 + 2.24) = 1.81 kNm

With b = 444 mm, D = 80 mm, $Z = bD^2/6$ = 0.474 x 10^6 mm^3 and

$\sigma_{bot} = M_{max}/Z$ = 3.82 MPa ∴ Cracking will not occur.

Maximum ultimate moment (ULS):

M^* = 0.8 (1.25M_{DL} + 2.0M_{LL}) = 3.60 kNm

< ϕM_u = 0.7 x 0.444 x 13.84 = 4.30 kNm ∴ ok

(ii) Taking moment resisting width of slab = 500+300 = 800mm

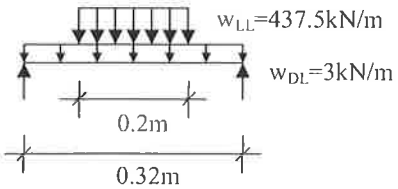

Maximum moment (SLS):

M_{max} = 0.8 (M_{DL} + M_{LL})

= 0.8 (0.04 + 4.81) = 3.88 kNm

* This width is selected to ensure that no cracking occurs in the deck due to transverse bending.

With b = 800 mm, D = 80 mm, $Z = bD^2/6$ = 0.853 x 10^6 mm^3 and

$\sigma_{bot} = M_{max}/Z$ = 4.55 MPa ∴ Cracking is unlikely (< 6.0 MPa).

Maximum ultimate moment (ULS):

$M^* = 0.8\ (1.25M_{DL} + 2.0M_{LL}) = 7.74$ kNm

$< \phi M_u = 0.7$ x (0.8 x 13.84) = 7.75 kNm $\therefore$ ok

- Check beam shear at d = 47.7mm from support. From (ii) with wheel load located 47.7mm from support: V^* = 95.0 kN; b = 800 mm; d = 47.7 mm and hence

$$\sigma_1 = \tau_{max} = \frac{V^* Q}{I\ b} = \frac{95\times10^3\times800\times40^2/2}{(800\times80^3/12)\times800} = 2.23\ \text{MPa} < (5.0+0.13\sqrt{f_c'})$$

- Check punching shear under wheel load:

V^* = 2.0 x 87.5 = 175.0 kN; d = 47.7 mm and u = 2(500+200+2x47.7) = 1591 mm. From Eqn 6.8 and taking σ_{cp}= 0, ϕV_{uo} = 265.6 kN > V^* $\therefore$ ok.

Longitudinal pretensioned ribs:

- Span = 1000 mm; w_{DL} = 1.53 kN/m.
- The load from one W7 wheel is
- assumed to be carried by 1.5 ribs.
- Max. +ve moment occurs with one W7 wheel load at midspan (200mm contact in direction of span) and = 70% of simply-supported moment.

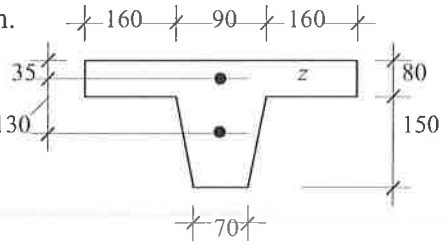

A = 44800 mm^2; $\bar{z}$ = 69.97 mm; I = 149.8 x 10^6 mm^4

- Max. –ve moment with a W7 wheel load in each of the adjacent spans = -65% of the simply-supported midspan moment.
- + ve $M_{max} = 0.7\ (M_{DL} + M_{LL})$

$= 0.7\ (0.19 + 13.13)$

$= 9.32$ kNm.

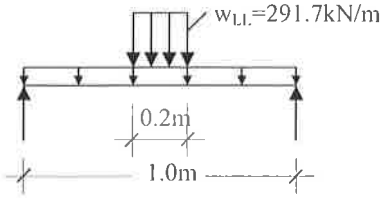

$\sigma_{bot} = M_{max}\ y/\ I$ = +9.95 MPa

The minimum residual compression due to prestress after all losses at the bottom fibre of the rib (from the stress distribution at the support in Step 6) is –4.23 MPa. Therefore, the maximum tensile stress in the bottom fibre of the rib is –4.23 + 9.95 = 5.72 MPa < 6.0 MPa. $\therefore$ ok.

- - ve $M_{max} = -0.65\ (M_{DL} + M_{LL}) = -8.65$ kNm.

$\sigma_{top} = M_{max}\ y/\ I$ = +4.04 MPa. The maximum tension in the top fibre occurs at the support (see stress distribution in Step 6) and equals +1.61 MPa. Therefore, the maximum tensile stress in the top fibre is +1.61 + 4.04 = 5.65 MPa < 6.0 MPa. $\therefore$ ok.

- At the ULS, the design +ve moment $M^* = 0.7\ (1.25M_{DL} + 2.0M_{LL}) = 18.50$ kNm. The ultimate moments for this pretensioned rib in +ve and –ve bending are calculated in accordance with Section 5 and are found to be $(M_u)_{+ve} = 34.6$ kNm and $(M_u)_{-ve} = 36.4$ kNm. The rib easily satisfies the requirements for flexural strength.

Transverse post-tensioned ribs:

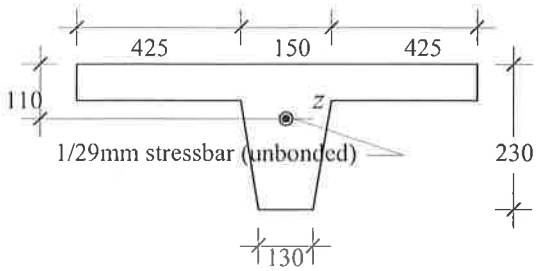

- Span = 1.62m;
- $w_{DL} = 3.01$ kN/m (includes longitudinal ribs).
- The load from one W7 wheel is carried by one rib.
- Max. +ve moment occurs with one W7 wheel load at midspan (500mm contact dimension in dirn of span) and equals 70% of the simply-supported midspan moment).

$A = 101000$ mm^2; $\bar{z} = 63.91$ mm; $I = 302.0 \times 10^6$ mm^4

- After all losses, the prestressing force in the unbonded bar is $P_e = 430$ kN at $d_p = 110$ mm ($e_p = 46.09$ mm) and the extreme fibre stresses due to P_e are $\sigma_{top} = -(P_e/A) + (P_e e_p/Z_t) = -0.07$ MPa and $\sigma_{bot} = -(P_e/A) - (P_e e_p/Z_t) = -15.16$ MPa.
- Serviceability Limit States:

  + ve $M_{max} = 0.8\ (M_{DL} + M_{LL}) = 0.8\ (0.99 + 29.97) = 24.77$ kNm and the resulting bottom fibre stress is

$$\sigma_{bot} = -15.16 + \frac{24.77 \times 10^6 \times 166.09}{302.0 \times 10^6} = -1.54 \text{ MPa.}$$

  - ve $M_{max} = 0.7\ (M_{DL} + M_{LL}) = 21.67$ kNm and the resulting top fibre stress is $\sigma_{top} = -0.07 + \dfrac{21.67 \times 10^6 \times 63.91}{302.0 \times 10^6} = +4.52$ MPa $<$ 6.0 MPa. $\therefore$ ok.

  The transverse rib will not crack under service loads.
- Ultimate Limit States:

  + ve $M^* = 0.75\ (1.25M_{DL} + 2.0M_{LL}) = 45.88$ kNm. The ultimate strength of this post-tensioned (but unreinforced) section in positive bending is $M_u = 66.0$ kNm and hence $\phi M_u = 0.7 \times 66.0 = 46.20$ kNm $> M^*$ $\therefore$ ok.

  - ve $M^* = 0.75\ (1.25M_{DL} + 2.0M_{LL}) = 45.88$ kNm. The ultimate strength of this post-tensioned (but unreinforced) section in negative bending is $M_u = 106.0$ kNm and hence $\phi M_u = 74.2$ kNm $> M^*$ $\therefore$ ok.

- Check dry joint between girders:

  Span = 0.78m. Maximum +ve moment at joint occurs when one W7 wheel load is applied at midspan directly over dry joint.

  + ve $M_{max} = 0.8\ (M_{DL} + M_{LL}) = 0.8\ (0.23 + 11.59) = 9.46$ kNm and the resulting top and bottom fibre concrete stresses are

$$\sigma_{bot} = -15.16 + \frac{9.46\times10^6 \times 166.09}{302.0\times10^6} = -9.95\ \text{MPa}$$

$$\sigma_{top} = -0.07 + \frac{9.46\times10^6 \times 63.91}{302.0\times10^6} = -2.07\ \text{MPa}$$

  Therefore, no tension will exist across the dry joint under service loads.

13. Design of anchorage zone:

The stress resultant forces away from the anchorage zone (assuming prestressing forces at transfer of 1370 kN in top strands at d_p = 100mm and 8624 kN in bottom strands at d_p = 100mm)) are as follows:

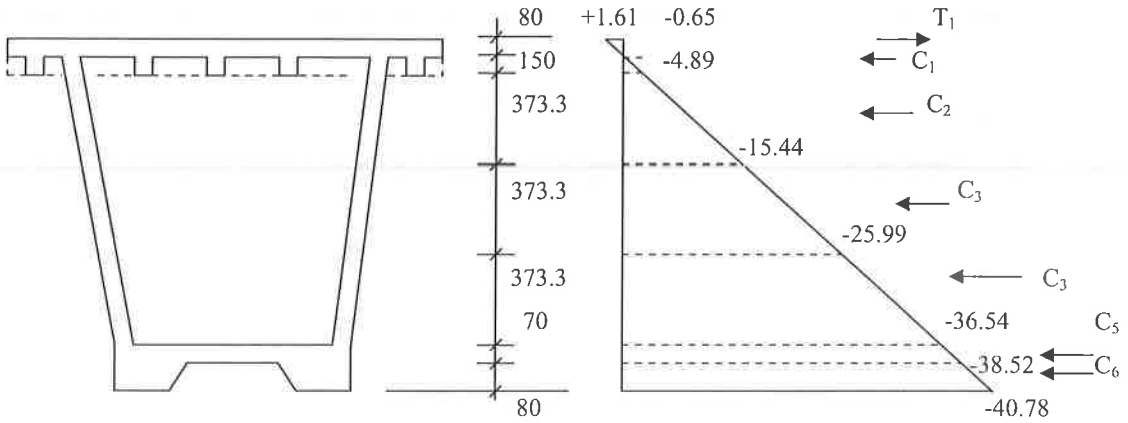

T_1 = 92.2 kN at d_{T1} = 8.6mm; C_1 = 224.4 kN at d_{C1} = 174.1mm; C_2 = 531.3 kN at d_{C2} = 449.0mm; C_3 = 1082.7 kN at d_{C3} = 805.8mm; C_4 = 1634.1 kN at d_{C4} = 1173.8mm; C_5 = 3415.2 kN at d_{C5} = 1385.3mm; C_6 = 2220.4 kN at d_{C6} = 1460.4mm.

Additional compressive forces representing the loss of prestress (due to elastic shortening) are located at the level of the top and bottom steel and are calculated as $(n\text{-}1)\sigma A_p$, where n is the modular ratio (= E_p/E_c = 5) and σ is the stress in the concrete at the steel level. These forces are C_{P1} = 4.9 kN and C_{P2} = 973.0 kN.

The strut and tie model shown below is based on stress contours obtained from an elastic finite element model of the anchorage zone and illustrates the flow of forces on an elevation of the beam.

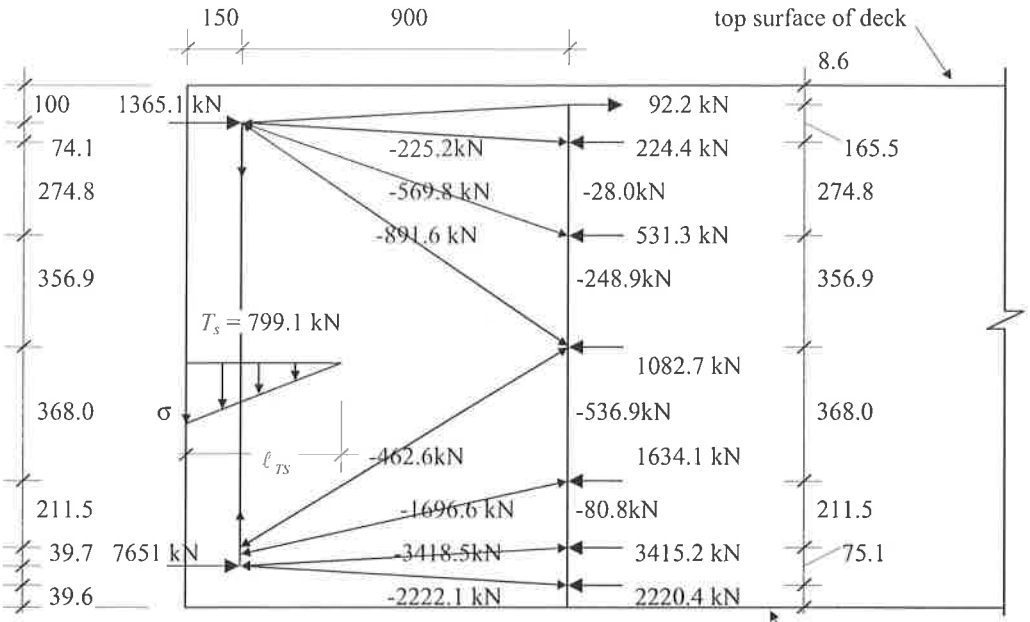

The tie T_s = 799.1 kN is located close to end face of the beam, with tensile stresses varying (approximately linearly) from a maximum at the end face to zero at about 400 mm in from the end face, as shown. With a web width of 2 x 70 = 140 mm, a linear elastic finite element analysis predicts a maximum tensile stress of about 35 MPa at the end face. Assuming T_s is carried by a linearly varying stress acting over an area $\ell_{TS} \times b_w$ (with σ_{max} = 8 MPa) and ℓ_{TS} is taken as $30d_b$ = 450mm, the required web thickness is

$$b_w = \frac{T_s}{0.5\sigma_{max}\ell_{TS}} = \frac{799.1\times10^3}{0.5\times8\times450} = 444 \text{ mm}$$

Increase the web thickness from 2 x 70mm to 2 x 220mm in the anchorage zone (within 1m from the end face). Alternatively, introduce a 100 mm thick diaphragm between the webs and centred on the tension tie force T_s, as indicated above.

A similar analysis is required to check the horizontal flow of forces in the slab base. A significant horizontal tension force exists within the bottom flange at the end face of the beam. Calculations show that an increase of the bottom flange thickness to at least 250 mm is required within the anchorage zone.